ISTANBUL TECHNICAL UNIVERSITY ★ FACULTY OF AERONAUTICS AND ASTRONAUTICS

FLIGHT DYNAMICS AND CONTROL OF THE CONVENTIONAL AIRCRAFT

GRADUATION PROJECT

Ahmet Kutsay DERE

Department of Aeronautical Engineering

Thesis Advisor: Dr. İsmail Bayezit

July, 2020

ISTANBUL TECHNICAL UNIVERSITY ★ FACULTY OF AERONAUTICS AND ASTRONAUTICS

FLIGHT DYNAMICS AND CONTROL OF THE CONVENTIONAL AIRCRAFT

GRADUATION PROJECT

Ahmet Kutsay DERE

Department of Aeronautical Engineering

Thesis Advisor: Dr. İsmail Bayezit

July, 2020

Ahmet Kutsay DERE, student of ITU Faculty of Aeronautics and Astronautics student ID **110150037**, successfully defended the graduation entitled **"FLIGHT DYNAMICS AND CONTROL OF THE CONVENTIONAL AIRCRAFT"**, which he prepared after fulfilling the requirements specified in the associated legislations before the jury whose signatures are below.

Thesis Advisor :	**Dr. İsmail Bayezit** Istanbul Technical University	.....
Jury Members :	**Prof Dr. Elbrus Caferov** Istanbul Technical University	.....
	Yrd. Doç. Dr. T. Berat Karyot Istanbul Technical University	.....
	Öğr. Gör. Dr. H. Barbaros Soyer Istanbul Technical University	.....
	Öğr. Gör. Dr. İsmail Bayezit Istanbul Technical University	.....

To my family,

Date of Submission : 13 July 2020

Date of Defense : 22 July 2020

FOREWORD

This thesis is about Modelling and Control of Quanser Inverted Pendulum Mechanism.

Dsdsfddfvc

Cv

xcvcxvcxv

July 2020 Name

TABLE OF CONTENTS

ABBREVIATIONS

SISO **:** Single Input-Single Output
SIMO **:** Single Input-Multi Output
MIMO **:** Multi Input-Multi Output

LIST OF TABLES

No table of figures entries found.

LIST OF FIGURES

No table of figures entries found.

LIST OF SYMBOLS

$\boldsymbol{R_m}$ **:** Motor Armature Resistance

$\boldsymbol{L_m}$ **:** Motor Armature Inductance

FLIGHT DYNAMICS AND CONTROL

OF THE CONVENTIONAL AIRCRAFT

SUMMARY

In this thesis, properties about Boeing 747 aircraft which have four turbofan engine intercontinental airliner aircraft were given. Thereafter, nonlineer Matlab-Simulink model of aircraft was given and simulation was demonstrated by using Simulink Blocks and Flight Gear Simulation Program. Finally, Stability Augmentation System and different sort of autopilot design were applied to model.

Matlab have lots of usefull tools and one of those, Control Design Tool, was used in Stability Augmentation System design. Linear Analysis Tool was used for obtaining state space matrices and by usign this matrices transfer function of each control surface to angular rates were obtained. By using rlocus function of Matlab, root locus graphics for each feedback loop were made draw and proper gain values were acquired. This feedbacks were applied on simulink model and step responses of case which with and without SAS were compared. Positive impact of stability augmentation was seen with comparison. The Automatic Flight Control book of Bernard Lewis and last bachelors graduate thesis was helpful.

Three autopilot design were made in this thesis. These are, Pitch Hold Autopilot, Altitude Hold Autopilot and Roll Angle Hold Autopilot. This autopilot design were made by using PID controller and implementing feedback with gain coefficient which is obtained from root locus graphics.

GELENEKSEL BİR YOLCU UÇAĞININ

UÇUŞ DİNAMİĞİ VE KONTROLÜ

ÖZET

Bu tezde 4 adet turbofan motoruna sahip kıtalararası bir yolcu uçağı olan Boeing 747 uçağı ile alakalı bilgiler verilmiş, sonrasında uçağın MATLAB-Simulink yazılımı kullanılarak modellenmesi, Simulink blokları ve Flight Gear Simülasyon programı ile simülasyonu ve uçağa ait kararlılığın artırımı (SAS) ve çeşitli otopilotların tasarımı uygulanmıştır.

Kararlılık artırımı uygulamasında Matlabda bulunan Control Design-Linear Analysis aracı kullanılmış, buradan elde edilen durum uzay matrisleri kullanılarak transfer fonksiyonları elde edilmiştir. Elde edilen transfer fonksiyonlarının root locus grafikleri çizdirilerek her bir geri besleme için uygun kazanç katsayıları elde edilmiş ve geri besleme simulink üzerinde doğrusal olmayan modele uygulanmış, kararlılık artırımının mevcut olduğu ve olmadığı durumlardaki sonuçlar kıyaslanmıştır. Kıyaslama ile kararlılık artırımının olumlu etkisi görülmüştür. Kararlılık artırımı uygulamasında Lewis in Automatic Flight Control kitabından ve geçmiş lisans mezuniyet tezlerinden faydalanılmıştır.

Otopilot tasarımında üç adet otopilot tasarımı yapılmıştır. Bunlar Yunuslama Açısı Sabitleme Otopilotu (Pitch Hold Autopilot), Yükseklik Sabitleme Otopilotu (Altitude Hold Autopilot) ve Yuvarlanma Açısı Sabitleme Otopilotudur (Roll Angle Hold Autopilot). Yapılan otopilot tasarımları root locus grafiği kullanılarak elde edilen kazanç katsayıları ile geri beslemeler yaparak ve PID kontrolcüler kullanılarak yapılmıştır.

1 INTRODUCTION

In this thesis, derivation of equations of motion, atmosphere model obtaining and modelling on matlab Simulink are implemented. Thereafter, stability augmentation and autopilot design for a manned aircraft are introduced.

In Chapter 2 some specifications of B747 are introduced. Besides, control surface limits and sign convention are shown.

In Chapter 3, how did Matlab-Simulink model of aircraft is expressed. In Chapter 3.1, firstly pilot inputs and actuator model are shown. In Chapter 3.2, total forces and moments which determine motion and attitude of aircraft are calculated and added to the full model. Total forces and moments are summation of three sub elements which are engine based, aerodinamic based and gravitation based forces and moments. Each impact are descripted in the subtitles and added to the full model.

In Chapter 3.3, construction of 6-DOF equation of motion in which is used total forces and moments. That equation of motion is constructed is added to the full model.

In Chapter 3.4, finally atmosphere model is constructed and added to the full model. With the addition of atmosphere model, 6-DOF nonlinear model of B747 had been obtained. In Chapter 3.5, simulink blocks which is used for simulation of aircraft model in Flight Gear are shown. In Chapter 3.6, demonstration blocks which is used for demonstration of results are descipted.

In Chapter 4, linearization and trimming of 6-DOF nonlinear model which is previously obtained and validated that it works properly are introduced and results are given.

In Chapter 5, by examining results which is obtained from linearization, it argued that whether SAS is needed or not.

In Chapter 6, as an alternative to SAS design, different autopilot designs are applied and results are given. In this part of thesis, three autopilot design are shown: Pitch Hold Autopilot, Altitude Hold Autopilot and Roll Angle Hold Autopilot.

In the last Chapter, Chapter 7, general evaluation about thesis and contribution of SAS and autopilot design is argued.

In Appendices, figures about simulink model and Matlab scripts which is used in this thesis are given.

Turkish version of this thesis and simulink model which is used in this thesis are accessible in the X website. I hope this graduation project is usefull for students which are interested in this subject.

2 AIRCRAFT PROPERTIES

In this part of the thesis Boeing 747 intercontinental passenger aircraft will be introduced and its technical properties and control surface deflection limits will be given. Besides, sign convention will also be introduced in this chapter.

2.1 Technical Properties of Aircraft

The first model of B747, B747-100 was firstly produced in 1969 and since then new member have attended 747 family. The properties of model used in this thesis are taken from reference X. Sarper Kumbasar Thesis. According to this reference B747 is an intercontinental four engine aircraft. Three view of aircraft and dimensions are shown in **Figure 1.**

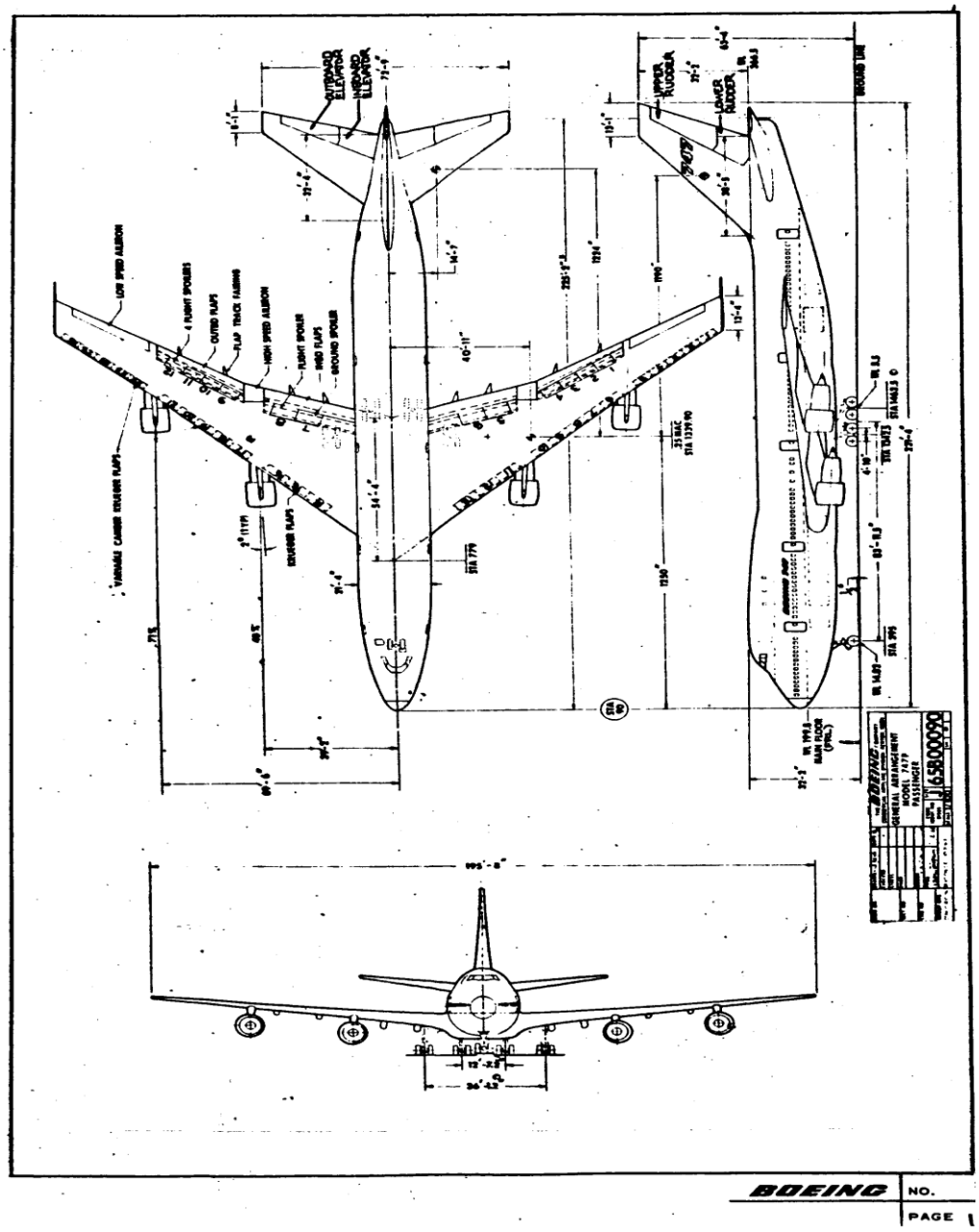

Figure 1. Three view of aircraft and dimensions

Some important specifications of aircraft used in simulation are shown in **Table 1.**

B747 Specifications	Dimensions
Wing Area	$5500\ \text{ft}^2$
Wing Mean Aerodynamic Chord	21.31 ft
Wing Span	195.68 ft
Center of Gravity	% 25 Mac
Airplane Gross Weight	600,000 lbf
Ix	$16.2 * 10^6\ slug * \text{ft}^2$
Iy	$33 * 10^6\ slug * \text{ft}^2$
Iz	$47.5 * 10^6\ slug * \text{ft}^2$
Ixz	$0.925 * 10^6\ slug * \text{ft}^2$
One Engine Thrust Force	43,500 lbf

Table 1. Some important specifications of aircraft used in simulation

2.2 Control Surfaces Limitations

Aircraft control surfaces could not be turned desired angle. There are angle limitations in positive and negative directions. Control surfaces limits which belongs to B747 are shown in **Table 2.**

Control Surface	Maximum Deflection Limits
Throttle	0 / 1
Elevator	-23 / +17
Aileron	-20 / +20
Rudder	-20 / +20

Table 2. . Control surfaces limits of B747

2.3 Sign Convention

Accepted positive directions on aircraft are shown in **Figure 2** which is taken from Reference X. According to this acceptation aircraft's nose direction is positive x, right wing direction is positive y direction and toward earth center is positive z direction. Around this positive axis, clock wise rotations are positive and reverse rotations are negative.

Reference X: Donald Mclean ın Automatic Flight Control Systems kitabından

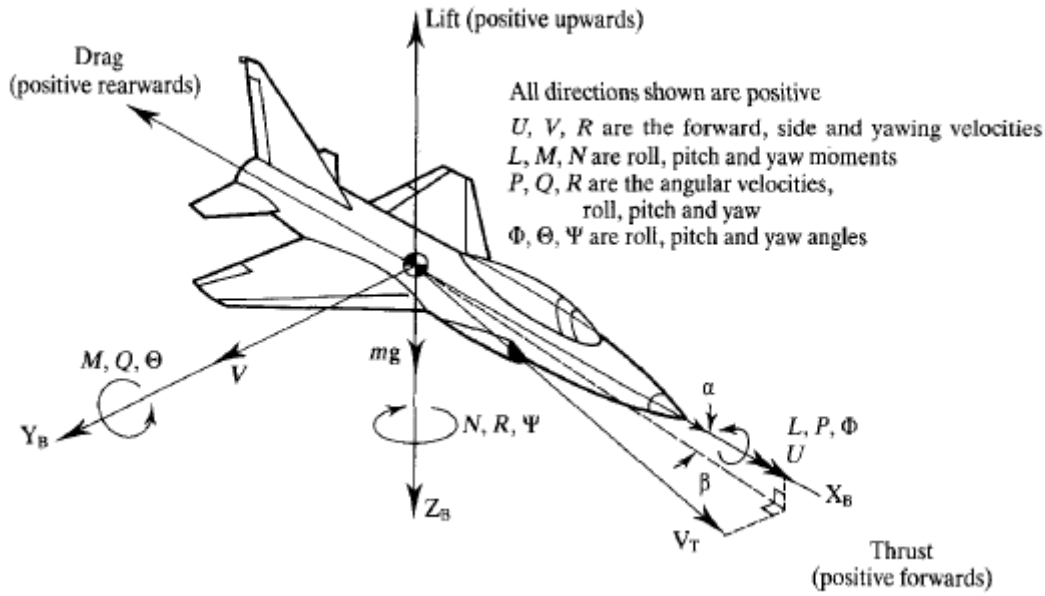

Figure 2. Sign Convention on Aircraft

As it can be seen in **Figure 3**, while positive rotation direction of elevator is downward, as a result of this movement aircraft is opposed to the nose down, negative pitching moment. Besides, positive angle of attack direction is also nose up direction. When it comes to ailerons, ailerons on each two wings work in reverse directions. While positive direction is upward for right aileron, it is downward for left aileron. When ailerons move to this position, aircraft is opposed to positive rolling moment. Finally, positive direction for rudder is toward to right. When rudder move this position aircraft is opposed to positive yawing moment.

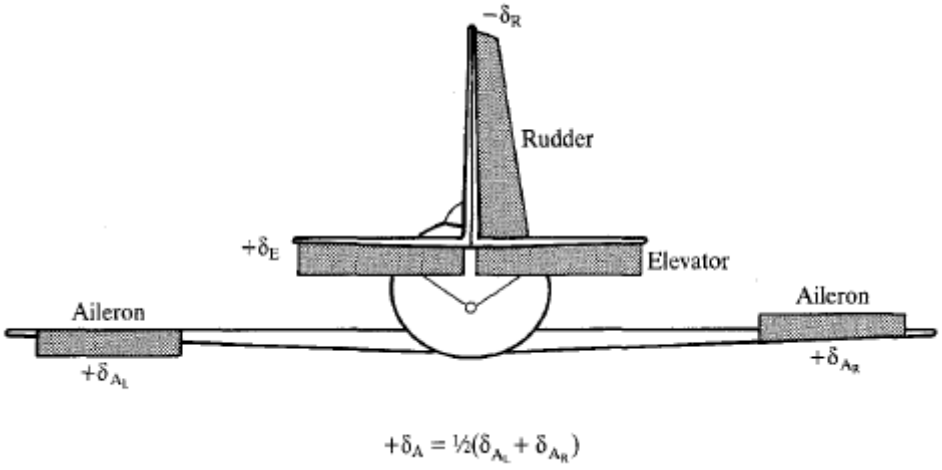

Figure 3. Positive Deflection Directions of Control Surfaces of Aircraft

Şekil X1 Donald McLean Sayfa6

3 PREPARATION FOR MODELLING

Some assumptions are made, while obtaining aircraft equation of motions on the purpose of attaining adequate precision in engineering and doing analysis with mathematical methods. Aircraft equation of motions are given in Chapter 4 with Simulink model. Each equation of motion are not obtained in detail instead taken equations from reference source are given. On the purpose of more understanding this equations, frames are introduced in this chapter.

3.1 Assumptions

While obtaining equation of motions 4 assumptions are made:

1. Assumption: Aircraft is a rigid body. Distance between two points of aircraft not change. Therefore, motion of aircraft can be described as translation motion of center of mass and rotation about center of mass.
2. Assumption: The mass of aircraft is constant. In real aircraft applications mass decreases due to fuel consumption. But this mass change is enough small to neglection.
3. Assumption: The aircraft is symmetric with respect to the XZ plane. Actually motion of control surface is not symmetric, thus aircraft has not an exact mass symmetry.
4. Assumption: The Earth is motionless in space. This assumption is based on reality of the rotation of Earth is negligibly small in problem which comprehend aircraft dynamics.

3.2 Flight Stability of an Aircraft

Stability is one of the most important phenomena for a controllable flight. Stability can be explained as return tendency to the original equilibrium state. The equilibrium states also can be explained as situation which total forces and moments on aircraft is equal zero. Stable aircrafts tend to return its equilibrium states when aircraft opposed to any disturbances. This disturbances can result from pilot or environmental effects. Thanks to stability, aircraft control becomes more easy than unstable aircraft without being controlled pilot command.

Stability and maneuverability are inversely proportional with each other. When one of these increase, the other decreases proportionally. For fighter aircraft increasing of

maneuverability is a design criteria, due to its mission performance. On the contrary, for the passenger aircraft the case is totally opposite. Increasing to stability is a design criteria for a passenger aircraft. Because the aim of commercial passenger aircraft is keep low to cost. Therefore most of the flight passes with cruise flight and it requires to stability.

Stability and maneuverability have a trade-off with each other. If stability increase too much, the control of aircraft become more difficult. Because aircraft does not respond to pilot command. On the contrary, if stability decrease too much, it means maneuverability is too high, aircraft keeps away from equilibrium states and keeping the aircraft at equilibrium states become difficult. Therefore adjusting balance between stability and maneuverability is an optimization problem.

The stability of an aircraft can be examine in two groups:

3.2.1 Static Stability

Static stability is the first tendency of aircraft to return equilibrium state. When any disturbances act on aircraft, aircraft can respond to disturbances three different way. If an aircraft is statically stable, it approaches to equilibrium states. If it is neutrally stable, it goes on its motion and this can be cause an accident. If it is statically unstable, it tend to increase effect of disturbances and far more moves away from equilibrium states.

One extra example for this phenomena can be shown in the **Figure 4**. In figure, behaviors of a spherical object are examined in three different situation. In each situation, object moves and its movement is observed.

At first part of the figure the object tends to return its original point. In that case, the object shows a statically stable or statically positive behaviour.

In the second part of the figure, the object keep away from its original position with an increasing speed. This case correspond to statically negative of statically unstable behavior.

At the last part of the figure the object tends to go on its movement along a straight line. If any other disturbance does not act on it, it would continue its motion until forever. In that case the movement of object characterizes the neutrally stable behavior.

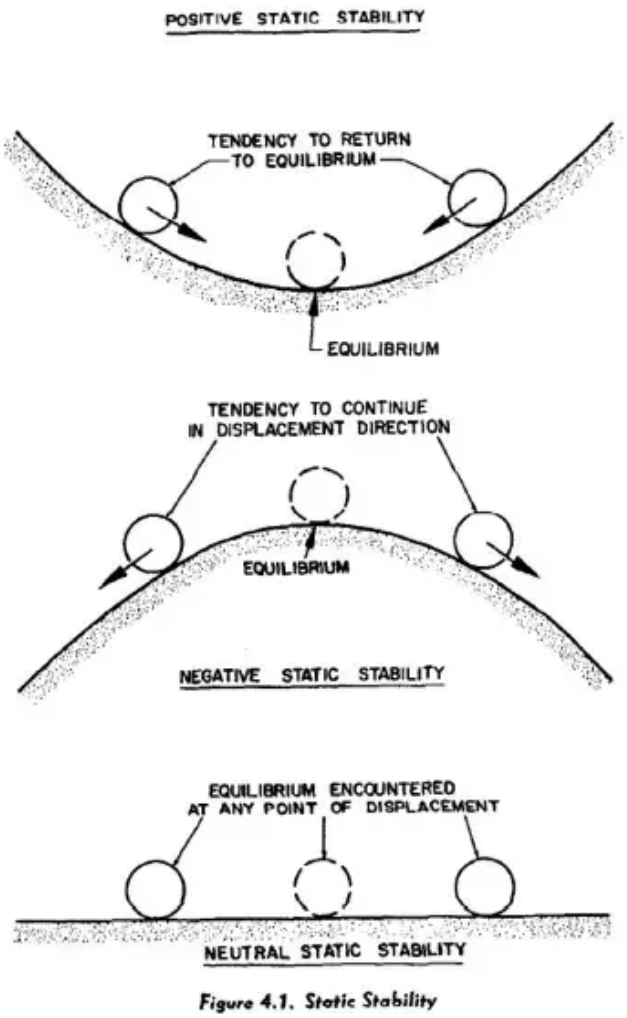

Figure 4. A Usefull Phenomena for Understanding Statci Stability

Three different kind of static stability can also be shown in **Figure 5.**

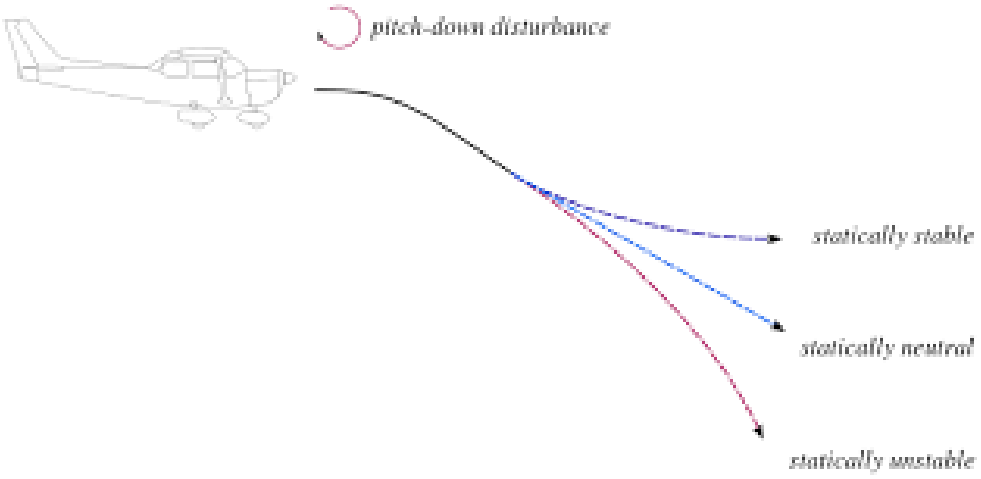

Figure 5. Static Stability Types on An Aircraft

3.2.2 Dynamic Stability

Dynamic stability means whether the aircraft reach or approach its equilibrium state or not. Figure X shows three different types of dynamic stability. In figure there are three aircrafts exposed same disturbances and acts different ways.

At the first part of the figure the aircraft approaches its equilibrium states by making an oscillation with an decreasing amplitude. This aircraft is said to have positive dynamic stability.

The second aircraft neither approaches nor moves away from equilibrium state. It makes a constant amplitude oscillation and this case is called as neutral dynamic stability.

At the last part of the figure the aircraft moves away from its equilibrium state by making an increasing amplitude oscillation. This behaviour is called dynamic instability or negative dynamic stability.

For each three states expressed above, the all aircrafts makes oscillation around a point. This means that the all aircrafts are statically stable. If they were statically unstable, they would not make oscillation as it can be seen in **Figure 6.**

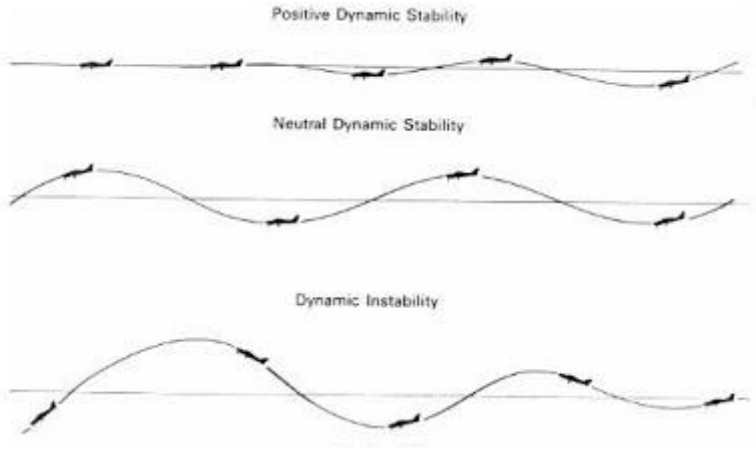

Figure 6. Figure 7. Dynamic Stability Types on An Aircraft

3.3 Frames and Transformations

On the purpose of more understanding different frames should be known. Firstly, the question of why different frames are needed should be answered. The aerodynamic forces and

moments which act on aircraft are obtained on stability frame and converted to body frame. The gravity forces are obtained on inertia frame and converted body frame. Aircraft velocities are acquired on body frame and this velocities are used in state space representation by converting to wind frame. Angular velocities are obtained on body frame. Transformation between frames are made by using Euler angles. As can be seen, different informations for aircraft model are attained in different frames and they should be transformed into one common frame. For this process, Euler angles are used.

3.3.1 Inertia Frame

The position states of aircraft, North-East-Down positions of aircraft, are calculated in inertia frame. Also gravity force are calculated in this frame and converted into the body frame.

Newton's second law is only valid for the inertial reference system. Therefore the inertia frame is accepted as a reference frame for aircraft applications. This acception is accurate for aircraft, because their speed of motion are highly big according to the rotation speed of Earth. Inertia frame which can also be called as North-East-Down (NED) frame is an Earth-fixed frame. The center of this frame located at a point on Earth. This point can be a ground control station or an airport tower. In this frame x direction shows North, y direction shows East and z direction shows center of the Earth. The Inertia frame can be seen **in Figure 8**.

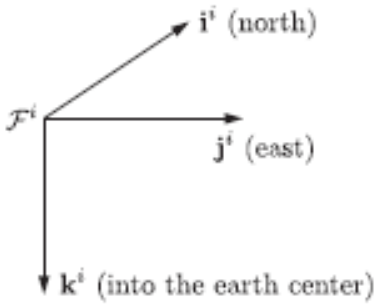

Figure 8. Inertia Frame

3.3.2 Body Frame

The velocities of aircraft which are in x, y and z direction as u, v, w are calculated in body frame and converted into wind frame as true air speed (Vt), angle of attack(α) and angle

of sideslip(β). The wind frame component are generally used as aircraft states rather than body frame velocities. Also thrust force and moments are calculated in this frame.

All calculations but position states are converted into this frame. Because all forces and moments act on aircraft and rotate or move it. Final impact of forces and moments are seemed on the aircraft body.

Body frame is located on the center of gravity of the aircraft. This frame is never change according to the aircraft. In this frame, x direction shows the nose of the aircraft, y direction lies through the right wing and z direction is perpendicular to x and y direction and This frame is position and attitude angles added version of inertia frame. The body frame can be shown in **Figure 9**.

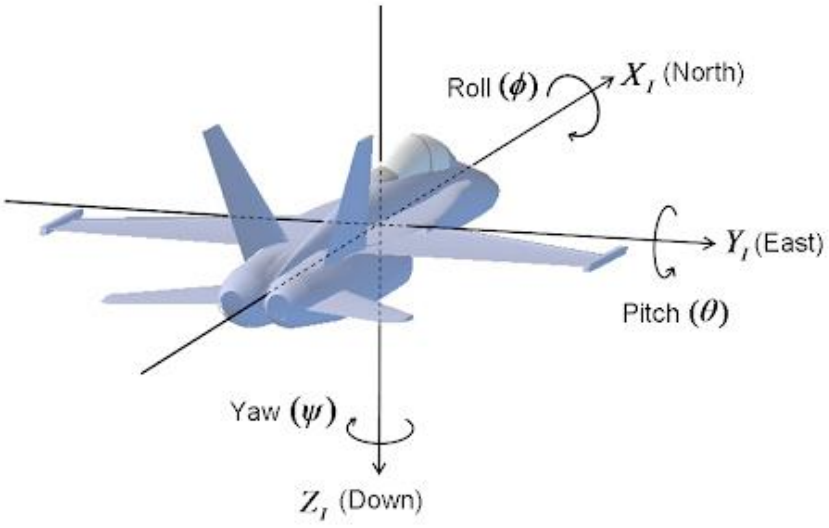

Figure 9. Body Frame

3.3.3 Stability Frame

In this frame, aerodynamic forces and moments are calculated and converted into the body frame of aircraft by using Euler angles.

Stability frame is obtained by rotating body frame up to angle of attack around y axis of body frame. Just as body frame, origin of stability frame is center of gravity of aircraft. X axis of this frame is rotated up to angle of attack x axis of body axis. Y axis lies through right wing of aircraft, it coincides with body frame y axis and z axis is perpendicular to this two axis and is in line bottom of the aircraft. The stability frame can be seen in FigureX.

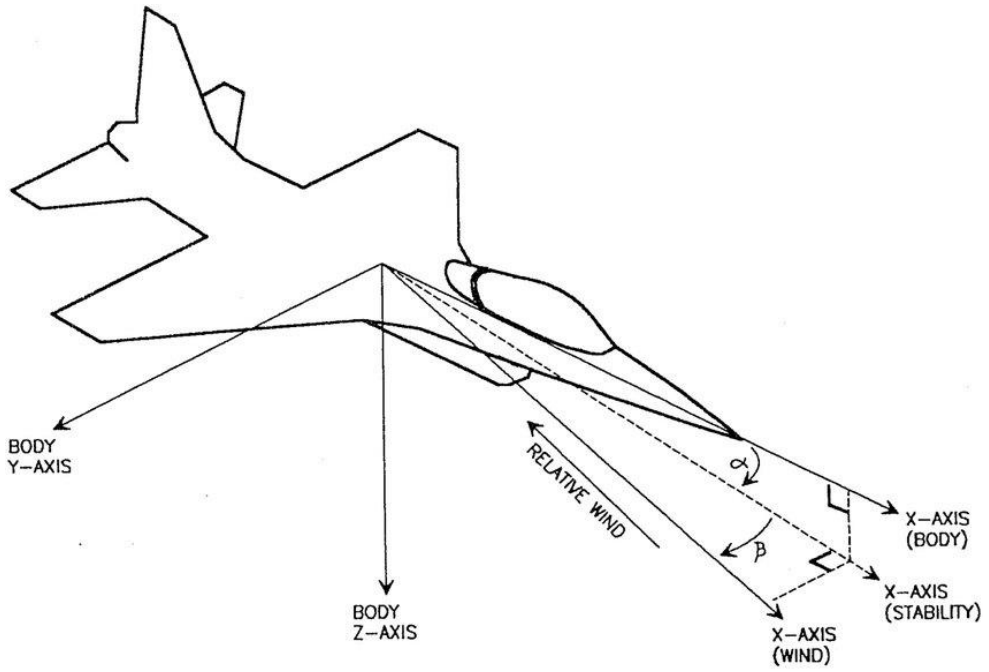

Figure 10. Stability Frame

3.3.4 Wind Frame

Wind frame is similar with stability frame and even if sideslip angle is zero, this two frame coincides with each other. Hence wind frame is rotated version of stability frame up to sideslip angle around y axis of body frame. Origin of this frame is aircraft's center of gravity, x axis lies toward the nose of aircraft but it is obtained by rotating body frame x axis up to angle of attack around y axis of body frame and sideslip angle around z axis of body frame. Y axis lies toward the right wing of aircraft but it is obtained by rotating body frame y axis up to sideslip angle around z axis of body frame. Z axis is perpendicular to this two axis and is in line bottom of the aircraft. Wind frame can be seen in Figure X with stability frame.

3.3.5 Transformations between Frames

As expressed in previous section different information are calculated in different frames and they have to be converted into one common frame via transformation matrices.

For instance gravity forces are expressed in the inertia frame. Because z axis of inertia frame is always toward the center of Earth and gravity vector too. The gravity force in inertia frame are shown in Equation X.

$$\vec{F}_{g,i} = \begin{bmatrix} 0 \\ 0 \\ W \end{bmatrix} = \begin{bmatrix} 0 \\ 0 \\ mg \end{bmatrix}$$

Aerodynamic forces and moments should be expressed into the stability frame or wind frame. Thus, lift force acts along the reverse z direction and drag force acts along the reverse x direction. The aerodynamic forces expression in stability frame can be seen in Equation X.

$$\vec{F}_{aero,st} = \begin{bmatrix} -D \\ F_{A_y} \\ -L \end{bmatrix}$$

Thrust forces should be expressed in the body frame. The thrust forces expression in body frame can be seen in Equation X.

$$\vec{F}_{thrust,bd} = \begin{bmatrix} T cos\emptyset_T \\ 0 \\ -T sin\emptyset_T \end{bmatrix}$$

While equations of motion are obtaining, frame transformations are needed to express all forces in same frame.

To transform a vector from inertia frame to body frame, it is have to respectively converted around z, y axis and x axis transform. Euler angles are used to transform a vector from inertia frame to body frame in flight dynamics. Euler angles are expressed as yaw(φ), pitch(θ) and roll($\emptyset$) angles. This angles are highly beneficial for orientation determination of aircraft. In **Figure 11,** usage order of Euler angles are shown.

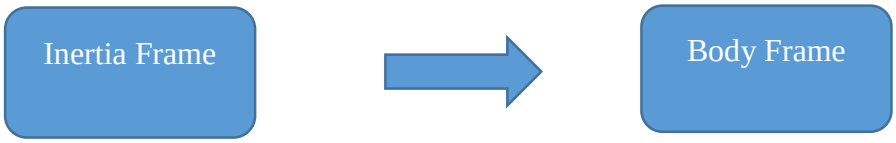

Figure 11. Inertia Frame to Body Frame Transformation

Allowed range of Euler angles are shown in Equation X.

$$0 \leq \varphi \leq 360\ [deg]$$

$$-90 \leq \theta \leq 90\ [deg]$$

$$-180 \leq \emptyset \leq 180 \ [deg]$$

Order of Euler angle rotations are highly important. If rotation are applied in different order, the result will be wrong. Obtaining process of rotation matrice which enable to transformation from inertia frame to body frame in Equation X, X1, X2, X3 and X4. Through this process two different dummy frame will be described as vehicle1 and vehicle2.

$$\vec{F}_i = \begin{bmatrix} X_i \\ Y_i \\ Z_i \end{bmatrix}$$

When F_i is respectively rotated up to φ, θ, $\emptyset$ angles around axis, the rotation matrices in X1,X2,X3 are obtained.

$$\begin{bmatrix} X_{v1} \\ Y_{v1} \\ Z_{v1} \end{bmatrix} = \begin{bmatrix} cos\varphi & sin\varphi & 0 \\ -sin\varphi & cos\varphi & 0 \\ 0 & 0 & 1 \end{bmatrix} \begin{bmatrix} X_i \\ Y_i \\ Z_i \end{bmatrix}$$

$$\begin{bmatrix} X_{v2} \\ Y_{v2} \\ Z_{v2} \end{bmatrix} = \begin{bmatrix} cos\theta & 0 & -sin\theta \\ 0 & 1 & 0 \\ sin\theta & 0 & cos\theta \end{bmatrix} \begin{bmatrix} X_{v1} \\ Y_{v1} \\ Z_{v1} \end{bmatrix}$$

$$\begin{bmatrix} X_{bd} \\ Y_{bd} \\ Z_{bd} \end{bmatrix} = \begin{bmatrix} 1 & 0 & 0 \\ 0 & cos\emptyset & sin\emptyset \\ 0 & -sin\emptyset & cos\emptyset \end{bmatrix} \begin{bmatrix} X_{v2} \\ Y_{v2} \\ Z_{v2} \end{bmatrix}$$

These three rotation matrices are respectively expressed as $R_1(\varphi)$, $R_2(\theta)$ and $R_3(\emptyset)$ the equation which transform a inertia frame matrix to body frame matrix are obtained.

$$F_{bd} = R_3(\emptyset)R_2(\theta)R_1(\varphi)\, F_i$$

This transformation matrix can be used to transform gravity forces from inertia frame to body frame.

$$\vec{F}_{gravity,i} = \begin{bmatrix} 0 \\ 0 \\ W \end{bmatrix} = \begin{bmatrix} 0 \\ 0 \\ mg \end{bmatrix}$$

$$\vec{F}_{gravity,bd} = \begin{bmatrix} 1 & 0 & 0 \\ 0 & cos\emptyset & sin\emptyset \\ 0 & -sin\emptyset & cos\emptyset \end{bmatrix} \begin{bmatrix} cos\theta & 0 & -sin\theta \\ 0 & 1 & 0 \\ sin\theta & 0 & cos\theta \end{bmatrix} \begin{bmatrix} cos\varphi & sin\varphi & 0 \\ -sin\varphi & cos\varphi & 0 \\ 0 & 0 & 1 \end{bmatrix} \begin{bmatrix} 0 \\ 0 \\ mg \end{bmatrix}$$

$$\vec{F}_{gravity,bd} = \begin{bmatrix} -mgsin\theta \\ mgsin\emptyset cos\theta \\ mgcos\emptyset cos\theta \end{bmatrix}$$

If transformation from body frame to inertia frame is needed, body frame matrix is respectively up to -∅, $-\theta$ and $-\varphi$. This transformation is shown X, X1, and X2.

$$F_i = R_1(-\varphi)R_2(-\theta)R_3(-\emptyset)\, F_{bd}$$

Because R_1, R_2 and R_3 are orthogonal matrix, relationship like X are accurate. So, transformation from body to inertia matrix can be writed as X1.

$$R_1(-\varphi) = {R_1}^T(\varphi)$$

$$R_2(-\theta) = {R_2}^T(\theta)$$

$$R_3(-\emptyset) = {R_3}^T(\emptyset)$$

$$F_i = {R_1}^T(\varphi){R_2}^T(\theta)\, {R_3}^T(\emptyset)F_{bd}$$

Stability frame to body frame transformation is highly important, due to aerodynamic force and moments. As can be seen in **Figure 12**, a vector can be transformed from stability frame to body frame by rotating up to a positive angle of attack. This transformation made with α angle around y axis or $R(\alpha)$ matrix.

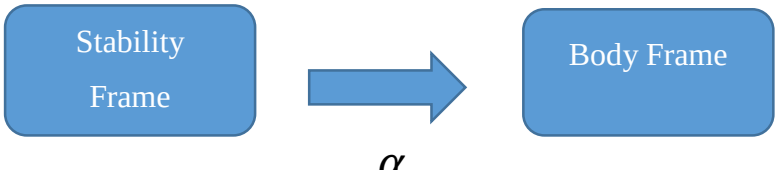

Figure 12. Stability Frame to Body Frame Transformation

Tranformation of aerodynamic forces from stability axis to body axis is shown below.

$$F_{aero,bd} = R(\alpha)\, F_{aero,st}$$

$$F_{aero,bd} = \begin{bmatrix} cos\alpha & 0 & -sin\alpha \\ 0 & 1 & 0 \\ sin\alpha & 0 & cos\alpha \end{bmatrix} \begin{bmatrix} -D \\ F_{A_Y} \\ -L \end{bmatrix}$$

$$F_{A_{x,bd}} = -Dcos\alpha + Lsin\alpha$$

$$F_{A_{y,bd}} = F_{A_{y,st}}$$

$$F_{A_{z,bd}} = -Dsin\alpha - Lcos\alpha$$

Transformation from wind frame to body frame are made by using α and β angles. Rotation matrix is given in X and wind frame to body frame transformation are shown in **Figure 12**.

$$F_{aero,bd} = \begin{bmatrix} F_{A_{x,bd}} \\ F_{A_{Y,bd}} \\ F_{A_{z,bd}} \end{bmatrix} = \begin{bmatrix} cos\alpha cos\beta & -cos\alpha sin\beta & -sin\alpha \\ sin\beta & cos\beta & 0 \\ sin\alpha cos\beta & -sin\alpha & cos\alpha \end{bmatrix} \begin{bmatrix} F_{A_{x,w}} \\ F_{A_{Y,w}} \\ F_{A_{z,w}} \end{bmatrix}$$

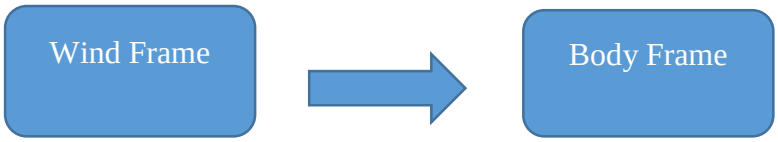

Figure 13. Wind Frame to Body Frame Transformation

$-\beta, \alpha$

In Figure X, all frame transformations are shown as a block schema. Arrow direction shows the positive transformation from one frame to another.

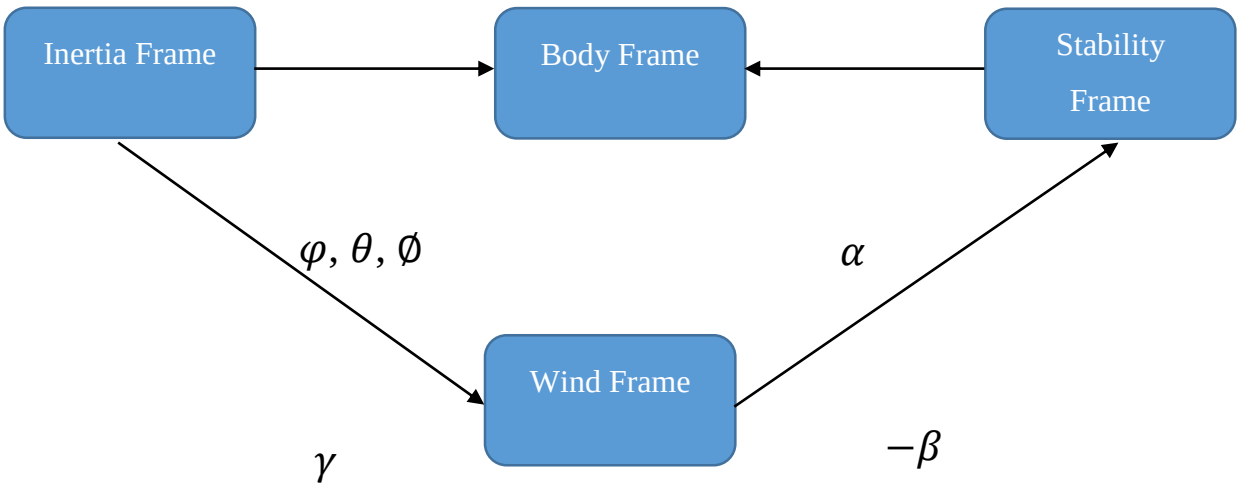

Figure 14. Transformations Among Frames

4

In many thesis and article aircraft modelling is made on Matlab-Simulink software. Because this tool is suitable for showing and manipulating all aircraft model all together. Thus, Matlab-Simulink software was used to install aircraft model in this thesis.

At the beginning, it is considered that demonstration of all model will be more clear in understanding of model. After demonstration of aircraft entire model, each subcomponent will be explained.

4.1 Pilot Model and SAS

Pilot command which is used in model composed of trimmed pilot inputs, saturation limits of throttle and all control surface deflection limits. In this block command input is obtained from workspace and then saturation limits applied them. In this part of model SAS feedbacks added to pilot command. The output is final pilot inputs. SAS will be explained later. Pilot Model and SAS can be seen in **Figure 15**.

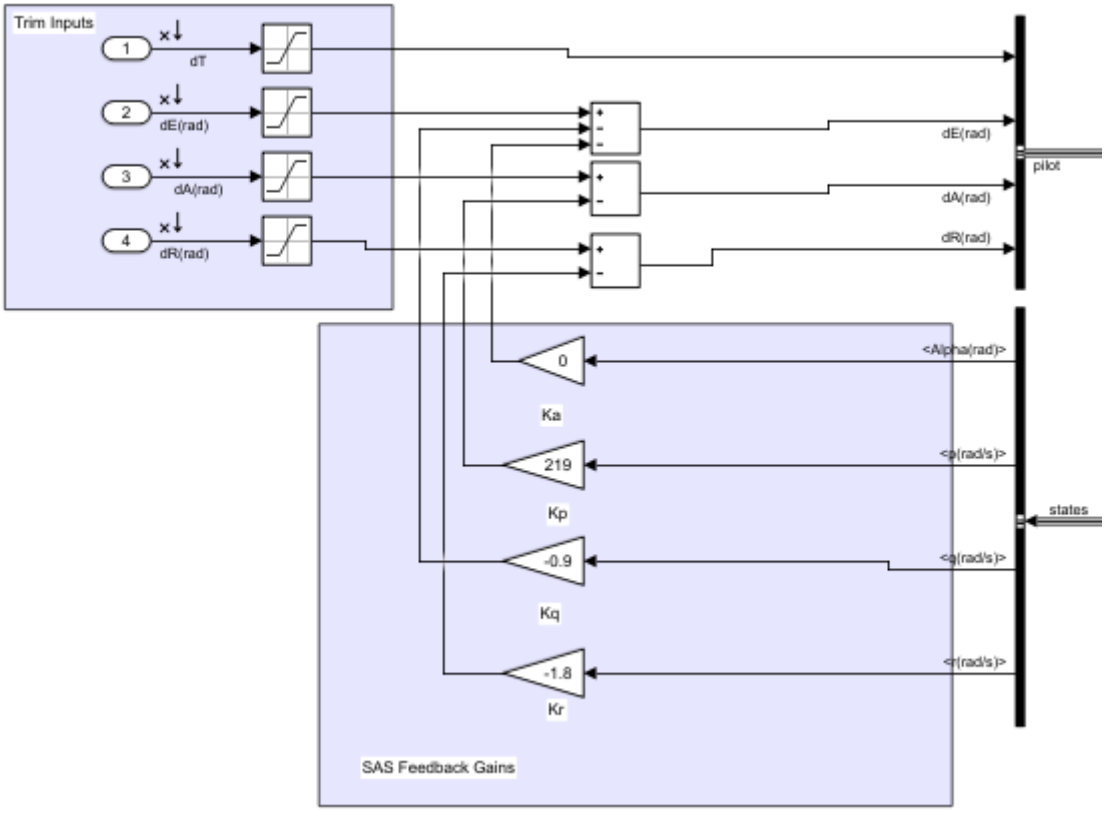

Figure 15. Pilot Model and SAS

4.2 Aircraft Dynamics

There are three subtitle in this chapter in which entire aircraft is modeled. This subtitles are total forces and moments, 6 DOF equation of motions and atmosphere model. In total forces and moment block, forces and moments determining motions of aircraft are calculated.

This forces and moments are used in equation of motions block and instant position, attitude, angular rate and velocity informations are calculated. In atmosphere model some atmospheric parameters needed for calculation of total forces and moments are calculated. Internal structure of aircraft dynamics block is shown in **Figure 16**. As can be seen in figure three mentioned system are in feedback form with each other.

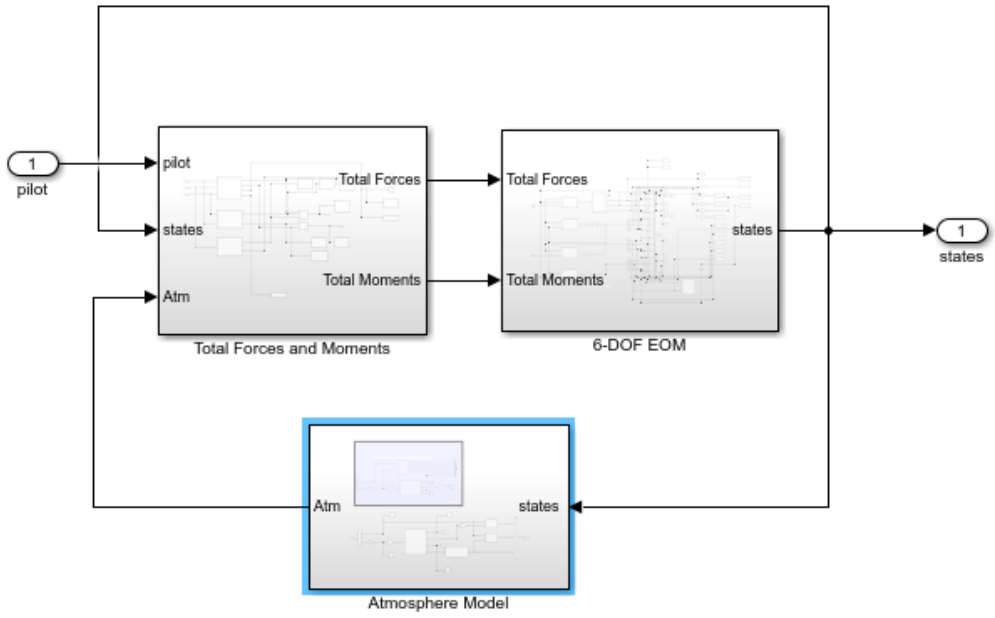

Figure 16. Internal Structure Of Aircraft Dynamics Block

4.2.1 Total Forces and Moments

In Total Forces and moment subsystem, pilot inputs, instant states and some atmospheric conditions are given as inputs and total forces and moments are calculated.

Total forces and moments are summation of engine, aerodynamic and gravity forces and moments. It can be seen in **Figure 17**. All forces and moments are three to one matrices and each row of these matrices stand out one axis component (X, Y, Z).

Although demonstration of Total Forces and Moment subsystem are made at this title, the inside of its subsystem are shown in appendices to avoid complexity in terms of appearance.

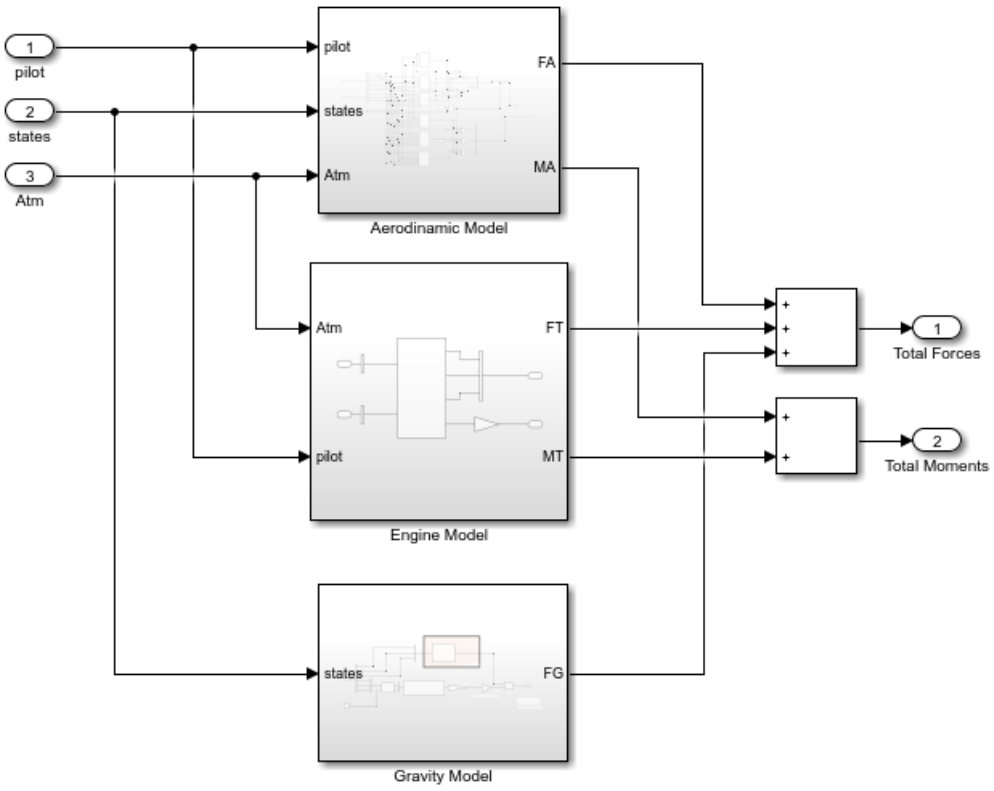

Figure 17. Internal Structure of Total Forces and Moments

4.2.1.1 Engine Model

The engine model of aircraft was taken from reference. X This model was updated and used in this model. The engine model takes density and throttle position as inputs and produce total force and moments which is resulted from engine. Calculation of forces and moments is used by matlab script and it will be given in appendices. The engine model of aircraft can also be seen in appendices. But some information about calculation thrust forces and moments is given in **Figure 18**. In this figure TmaxSL is maximum thrust force at sea level, σ is density ratio which is mean of density at the current altitude divided by sea level density. δ_T means that throttle deflection between 0 to 1.

$$F_{T_x} = T_{\max_{SL}} \sigma \delta_T \cos \phi_T$$

$$F_{T_z} = -T_{\max_{SL}} \sigma \delta_T \sin \phi_T$$

$$M_T = -T_{\max_{SL}} \sigma \delta_T d_T$$

Figure 18. Thrust Forces And Moments Equations

As it can be seen in the **Figure 19**, $\emptyset_T$ and d_T are respectively correspond to angle between thrust line and x direction of aircraft and distance between thrust line and x direction of aircraft, besides d_T can be called thrust moment arm.

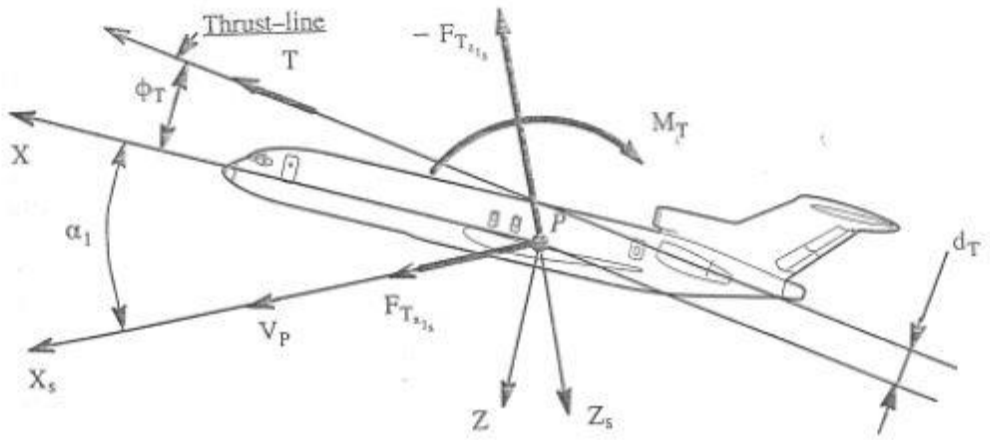

Figure 19.Demonstration of Thrust Force and Direction

The engine model is shown in Figure X. The script which calculates the thrust forces and moments is given in appendices.

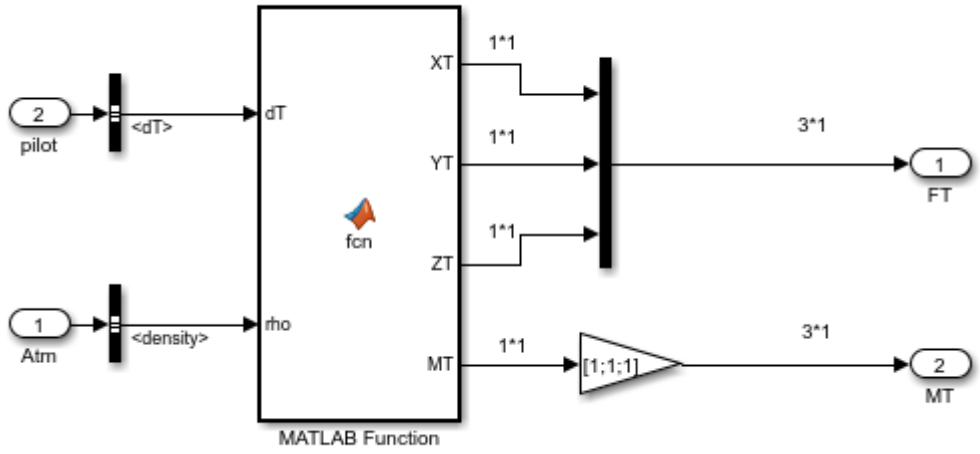

Figure 20. Internal Structure of Engine Model

Matlab function in Figure X, is given below.

```
function [XT,YT,ZT,MT] = fcn(dT,rho)

Tmax_SL=4*43500; % 43500 Ibf for each engine

rhoSL=0.002377; %(slug/ft^3)
phiT=deg2rad(0); % angle between engine and aircraft X axes
ema=0;%Engine Moment Arm
sigma=rho/rhoSL;
XT= Tmax_SL*sigma*dT*cos(phiT);     %Ibf
YT=0;                               %Ibf
ZT=-1*Tmax_SL*sigma*dT*sin(phiT);   %Ibf
MT =-1*Tmax_SL*sigma*dT*ema;        %Ibf*ft
```

4.2.1.2 Aerodinamic Model

The aerodynamic coefficient of an aircraft is hardly findable datas of an aircraft. So, B747 aerodynamic datas were searched for a long time. Finally D6-30463 numbered NASA report was found. The aerodynamic coefficient of B747 aircraft was taken from report NASA. This report include aerodynamic coefficient as graphically. Aerodynamic coeffiecients are used in model via lookup tables. Due to Aerodynamic model have lots of sub blocks, it is not explained in this thesis.

In this part of thesis each aerodynamic coefficient equation and its sub elements are explained. These equations also taken from NASA report.

Dimensionless Drag Force Coefficient

$$C_D = C_{DMach} + \Delta C_{Dsideslip} + \Delta C_{Drudder}$$

C_{DMach}: $Basic\ drag\ coefficient\ of\ the\ rigid\ aircraft$

$\Delta C_{Dsideslip}$: $Change\ in\ drag\ coefficient\ with\ respect\ to\ sideslip\ angle\ change$

$\Delta C_{Drudder}$: $Change\ in\ drag\ coefficient\ with\ respect\ to\ rudder\ angle\ change$

Dimensionless Side Force Coefficient

$$C_Y = \frac{dC_Y}{d\beta}\beta + \frac{dC_Y}{dr}\frac{r * b}{2 * Vt} + \frac{dC_Y}{dp}\frac{p * b}{2 * Vt} + \Delta C_{Yrudder}$$

$\frac{dC_Y}{d\beta}\beta$: $Change\ in\ side\ force\ coefficient\ with\ respect\ to\ the\ sideslip\ angle\ change$

$\frac{dC_Y}{dr}\frac{r * b}{2 * Vt}$: $Change\ in\ side\ force\ coefficient\ with\ respect\ to\ the\ yaw\ rate\ change$

$\frac{dC_Y}{dp}\frac{p * b}{2 * Vt}$: $Change\ in\ side\ force\ coefficient\ with\ respect\ to\ the\ roll\ rate\ change$

$\Delta C_{Yrudder}$: $Change\ in\ side\ force\ coefficient\ with\ respect\ to\ the\ rudder\ angle\ change$

Dimensionless Lift Force Coefficient

$$C_L = C_{Lbasic} + K_a\frac{dC_L}{d\delta_{ei}}\delta_{ei} + K_a\frac{dC_L}{d\delta_{eo}}\delta_{eo} + \frac{dC_L}{dq}\frac{q * c}{2 * Vt}$$

C_{Lbasic}: $Basic\ lift\ coefficient\ of\ the\ rigid\ aircraft$

$K_a\frac{dC_L}{d\delta_{ei}}\delta_{ei}$: $Change\ in\ lift\ coefficient\ with\ respect\ to\ inboard\ elevator\ angle\ change$

$K_a\frac{dC_L}{d\delta_{eo}}\delta_{eo}$: $Change\ in\ lift\ coefficient\ with\ respect\ to\ outboard\ elevator\ angle\ change$

$\frac{dC_L}{dq}\frac{q * c}{2 * Vt}$: $Change\ in\ lift\ coefficient\ with\ respect\ to\ pitch\ rate\ change$

Dimensionless Rolling Moment Coefficient

$$C_l = \frac{dC_l}{d\beta}\beta + \frac{dC_l}{dr}\frac{r * b}{2 * Vt} + \frac{dC_l}{dp}\frac{p * b}{2 * Vt} + \Delta C_{lrudder} + \Delta C_{l\_inbail}$$

$\frac{dC_l}{d\beta}\beta$: $Change\ in\ rolling\ moment\ coefficient\ with\ respect\ to\ the\ sideslip\ angle\ change$

$\frac{dC_l}{dr}\frac{r*b}{2*Vt}$: $Change\ in\ rolling\ moment\ coefficient\ with\ respect\ to\ the\ yaw\ rate\ change$

$\frac{dC_l}{dp}\frac{p*b}{2*Vt}$: $Change\ in\ rolling\ moment\ coefficient\ with\ respect\ to\ the\ roll\ rate\ change$

$\Delta C_{lrudder}$: $Change\ in\ rolling\ moment\ \ coefficient\ with\ respect\ to\ the\ rudder\ angle\ change$

$\Delta C_{l\_inbail} = Change\ in\ rolling\ moment\ \ coefficient\ with\ respect\ to\ the\ inboard\ aileron\ angle\ change$

Dimensionless Pitching Moment Coefficient

$$C_m = C_{m.25basic} + K_a\frac{dC_{m.25}}{d\delta_{ei}}\delta_{ei} + K_a\frac{dC_{m.25}}{d\delta_{eo}}\delta_{eo} + \Delta C_{m.25inbail} + \Delta C_{m.25sideslip} + \Delta C_{m.25rudder} + \frac{dC_m}{dq}\frac{q*c}{2*Vt}$$

$C_{m.25basic}$: $Basic\ lift\ coefficient\ of\ the\ rigid\ aircraft$

$K_a\frac{dC_{m.25}}{d\delta_{ei}}\delta_{ei}$: $Change\ in\ rolling\ moment\ coefficient\ with\ respect\ to\ inboard\ elevator\ angle\ change$

$K_a\frac{dC_{m.25}}{d\delta_{eo}}\delta_{eo}$: $Change\ in\ rolling\ moment\ coefficient\ with\ respect\ to\ outboard\ elevator\ angle\ change$

$\Delta C_{m.25inbail}$: $Change\ in\ pitching\ moment\ \ coefficient\ with\ inboard\ aileron\ angle\ change$

$\Delta C_{m.25sideslip}$: $Change\ in\ pitching\ moment\ coefficient\ with\ respect\ to\ sideslip\ angle\ change$

$\Delta C_{m.25rudder}$: $Change\ in\ pitching\ moment\ coefficient\ with\ respect\ to\ rudder\ angle\ change$

$\frac{dC_m}{dq}\frac{q*c}{2*Vt}$: $Change\ in\ pitching\ moment\ coefficient\ with\ respect\ to\ the\ pitch\ rate\ change$

Dimensionless Yawing Moment Coefficient

$$C_n = \frac{dC_n}{d\beta}\beta + \Delta C_{lrudder} + \Delta C_{l\_inbail}$$

$\frac{dC_n}{d\beta}\beta$: $Change\ in\ yawing\ moment\ coefficient\ with\ respect\ to\ the\ sideslip\ angle\ change$

$\Delta C_{lrudder}$: $Change\ in\ yawing\ moment\ \ coefficient\ with\ respect\ to\ the\ rudder\ angle\ change$

$\Delta C_{l\_inbail} = Change\ in\ yawing\ moment\ \ coefficient\ with\ respect\ to\ the\ inboard\ aileron\ angle\ change$

4.2.1.3 Gravity Model

In gravity model of aircraft, WGS84 Model was used. As stated in the Matworks website The WGS84 Gravity Model block implements the mathematical representation of the geocentric equipotential ellipsoid of the World Geodetic System (WGS84). [X]. This block takes position as latitude, longitude and altitude and produce output is the Earth's gravity at a specific location. At the entrance of this block, position comes from 6-DOF EOM block as inertial axis positions and it must be converted into earth geodetic locations. Thus, Flat Earth to LLA block is used for this purpose. This block have two input, first input is inertial axis positions and second is reference altitude. The reference altitude is choosed as sea level altitude, that is zero ft. Internal structure of gravity model can be seen in **Figure 21.**

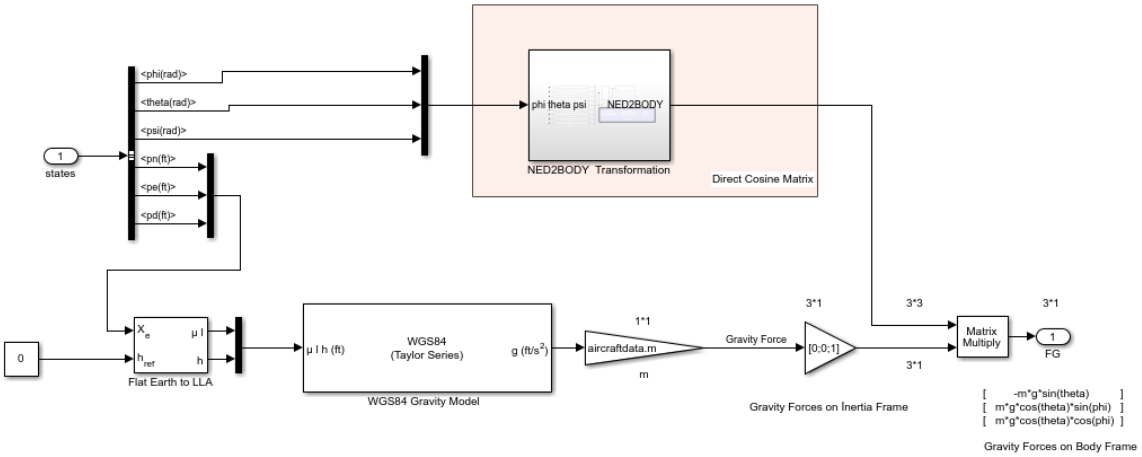

Figure 21. Internal Structure of Gravity Model

4.2.2 Atmosphere Model

The Atmosphere Model is used for calculate instant Mach number, density and dynamic pressure and this datas are used in other subsystems. The atmosphere model has two inputs. First input is velocity which is used for Mach number and dynamic pressure calculations. Other input is altitude which is input of ISA Atmosphere Model. The Simulink have different kind of atmosphere models such as ISA Atmosphere Model, COESA Atmosphere Model, CIRA-86 Atmosphere Model and NRLM-SISE 00 Atmosphere Model etc. In this report ISA Atmosphere Model is used. Due to this block takes altitude in meter, conversion is made from ft to meter at the entrance of blocks. And also conversion from meter

to ft is made, because the model is constructed with English Unit System. Internal Structure of atmosphere model can be seen in **Figure 22.**

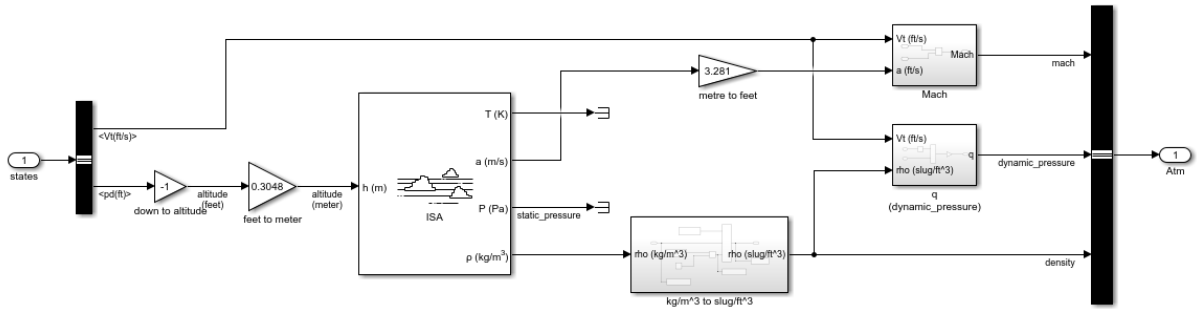

Figure 22. Internal Structure of Atmosphere Model

4.2.3 6-DOF Equation of Motion

The 6-DOF equation of motion subsystem is shown in **Figure 23**. As it can be seen in figure this subsystem only takes total forces and moments and calculates all states of aircraft. States are composed of 12 elements and it can be categorized into four groups.

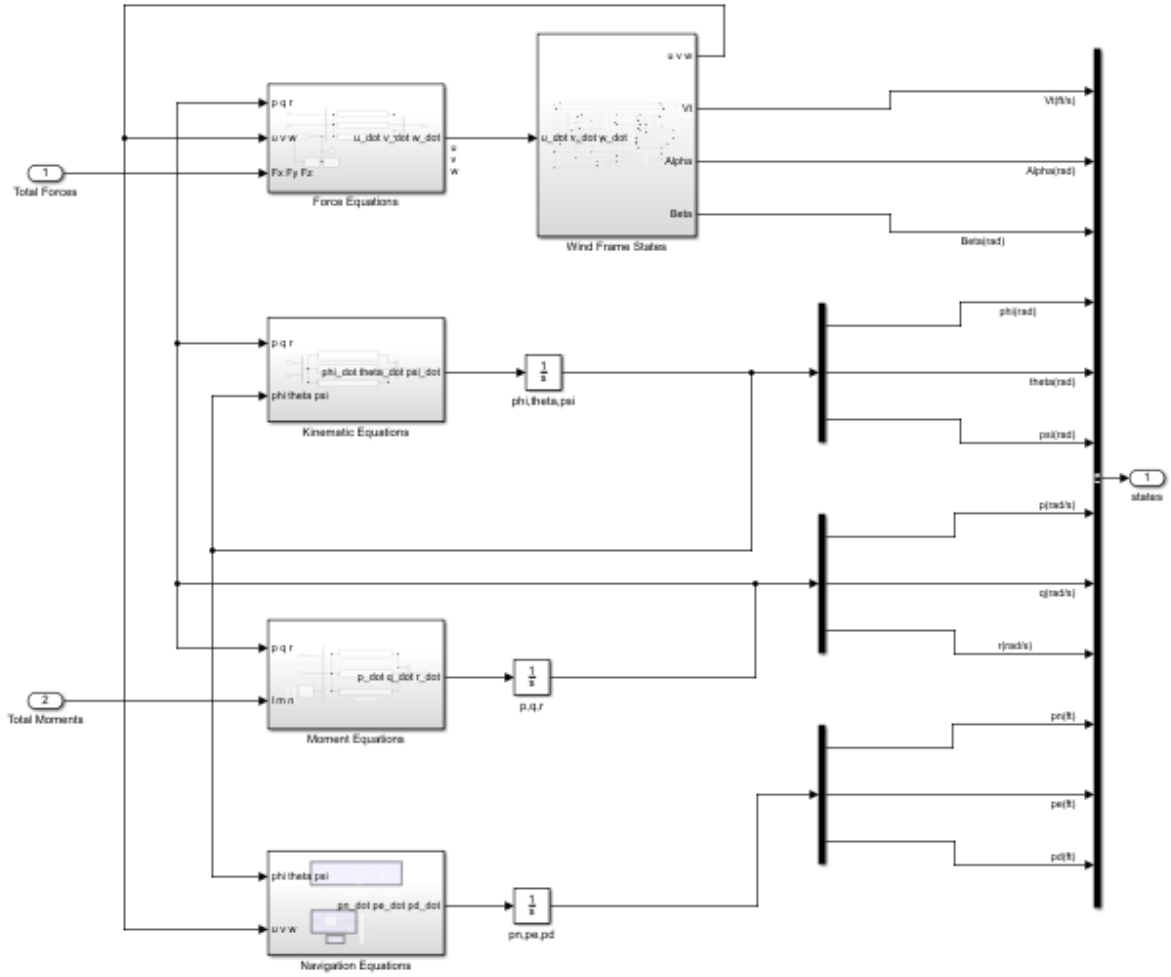

Figure 23. Internal Structure of 6 DOF EOM Model

4.2.3.1 Velocity Equations

This group includes velocity components of aircraft which are in body frame. This velocities are u, v, w which respectively correspond to x, y and z component of body velocity. They can be converted into wind axis frame as Vt which means true air speed, alpha means angle of attack and beta means sideslip angle.

The aircraft velocity equations are given as following equations-Equation X1, X2, X3. This equations are taken from reference X. In addition to this, the Simulink implementation of velocity equations is shown in **Figure 24**.

$$\dot{u} = r * v - q * w + \frac{F_x}{m}$$

$$\dot{v} = p * w - r * u + \frac{F_y}{m}$$

$$\dot{w} = q * u - p * v + \frac{F_z}{m}$$

Reference X: Randal Beard

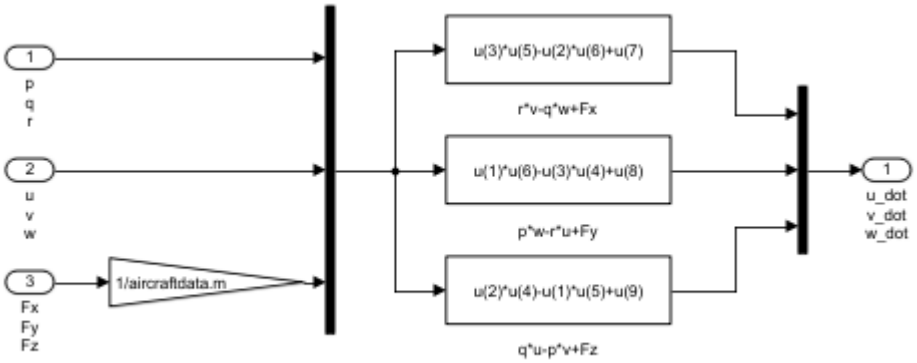

Figure 24. The Simulink Implementation Of Velocity Equations

4.2.3.2 Euler Angles Equations

This group which includes attitude of aircraft are composed of roll angle, pitch angle and yaw angle of aircraft. This angles are defined previously in Chapter 3, frames and conversion title.

The aircraft Euler angles equations are given as following equations-Equation X1,X2,X3. This equations are taken from reference X. In addition to this, the Simulink implementation of Euler angles equations is shown in **Figure 25**.

$$\dot{phi} = p + \tan(theta) * [q * \sin(phi) + r * \cos(phi)]$$

$$\dot{theta} = q * \cos(phi) - r * \sin(phi)$$

$$\dot{psi} = [q * \sin(phi) + r * \cos(phi)] * \sec(theta)$$

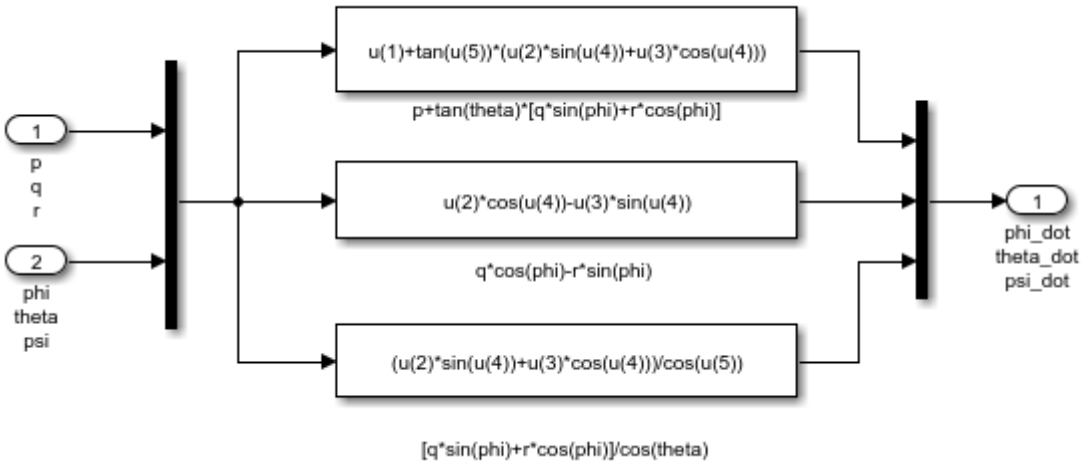

Figure 25. The Simulink Implementation Of Euler Angles Equations

4.2.3.3 Angular Rates Equations

The Angular rates can be regarded as changing rate of Euler angles. The aircraft angular rate equations are given as following equations-Equation X1, X2, X3. This equations are taken from reference X. In addition to this, the Simulink implementation of angular rates equations is shown in **Figure 26**.

$$\dot{p} = C_1 * p * r - C_2 * q * r + C_3 * l + C_4 * n$$

$$\dot{q} = C_5 * p * r - C_6 * (p^2 - r^2) + \frac{1}{I_{yy}} * m$$

$$\dot{r} = C_7 * p * q - C_1 * q * r + C_4 * l + C_8 * n$$

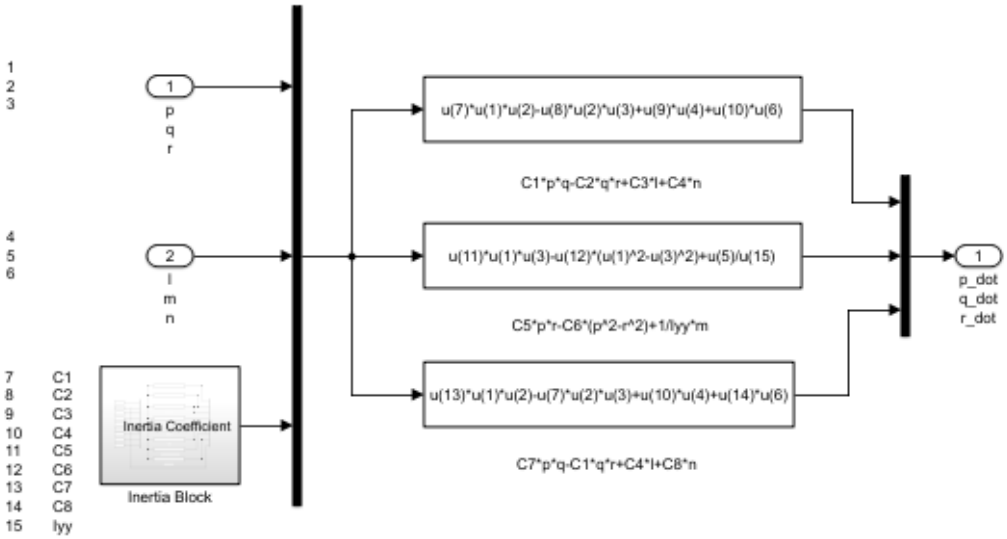

Figure 26. The Simulink Implementation Of Angular Rates Equations

In Figure X, eight coefficients can be seen in Inertia Block. This coefficients are derived from inertia coefficients and each coefficient are explained below. Also, inside of Inertia block can be seen in **Figure 27**.

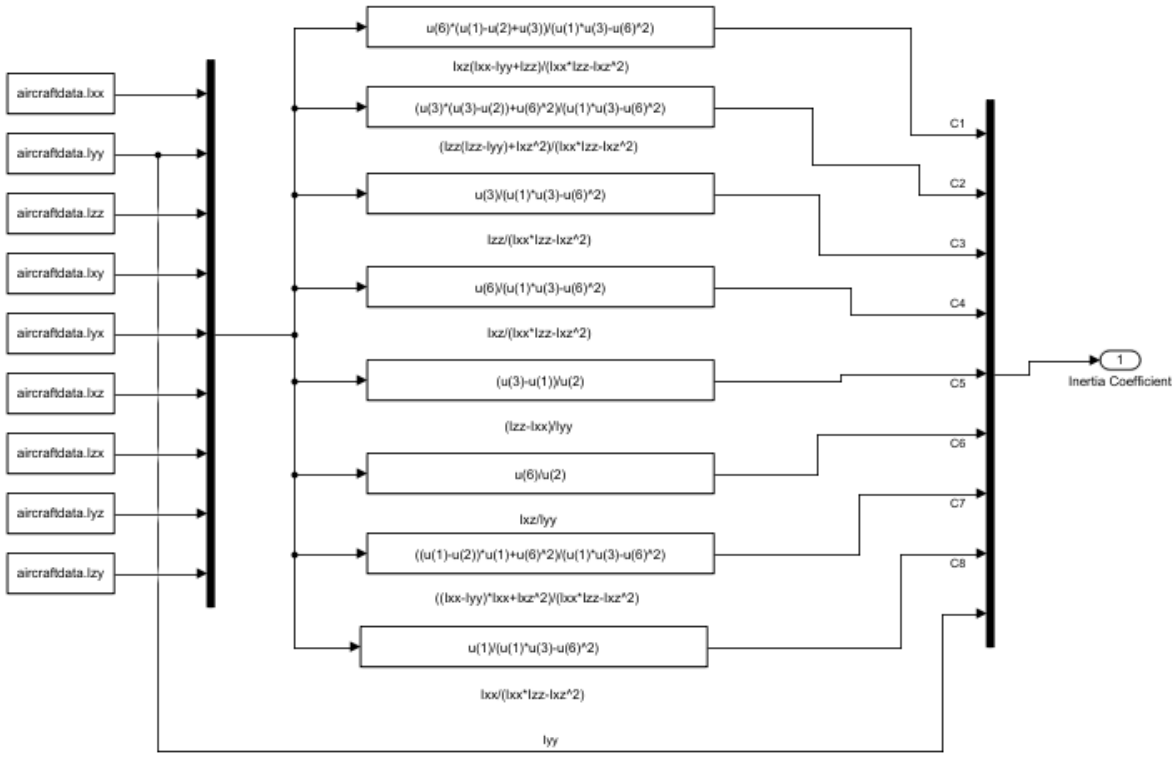

Figure 27. Inside Of Inertia Block

$$C = I_x * I_z - {I_{xz}}^2$$

$$C_1 = \frac{I_{xz} * (I_{xx} - I_{yy} + I_{zz})}{C}$$

$$C_2 = \frac{I_{zz} * (I_{zz} - I_{yy}) + {I_{xz}}^2}{C}$$

$$C_3 = \frac{I_{zz}}{C}$$

$$C_4 = \frac{I_{xz}}{C}$$

$$C_5 = \frac{I_{zz} - I_{xx}}{I_{yy}}$$

$$C_6 = \frac{I_{xz}}{I_{yy}}$$

$$C_7 = \frac{(I_{xx} - I_{yy}) * I_{xx} + {I_{xz}}^2}{C}$$

$$C_8 = \frac{I_{xx}}{C}$$

4.2.3.4 Position Equations

In this block position of aircraft in inertial frame are calculated by using body velocities and Euler angles.

The aircraft position equations are given as following equations - Equation X1, X2, X3. This equations are taken from reference X. In addition to this, the Simulink implementation of angular rates equations is shown in **Figure 28.**

$$\dot{pn} = u * \cos(theta) * \cos(psi) - \mathrm{v} * [\sin(phi) * \sin(theta) * \cos(psi) - \cos(phi) * \sin(psi)] + \mathrm{w} * [\cos(phi) * \sin(theta) * \cos(psi) + \sin(phi) * \sin(psi)]$$

$$\dot{pd} = u * \cos(theta) * \sin(psi) + \mathrm{v} * [\sin(phi) * \sin(theta) * \sin(psi) + \cos(phi) * \cos(psi)] + \mathrm{w} * [\cos(phi) * \sin(theta) * \sin(psi) - \sin(phi) * \cos(psi)]$$

$$\dot{pe} = -\sin(theta) + v * \sin(phi) * \cos(theta) + w * \cos(phi) * \cos(theta)$$

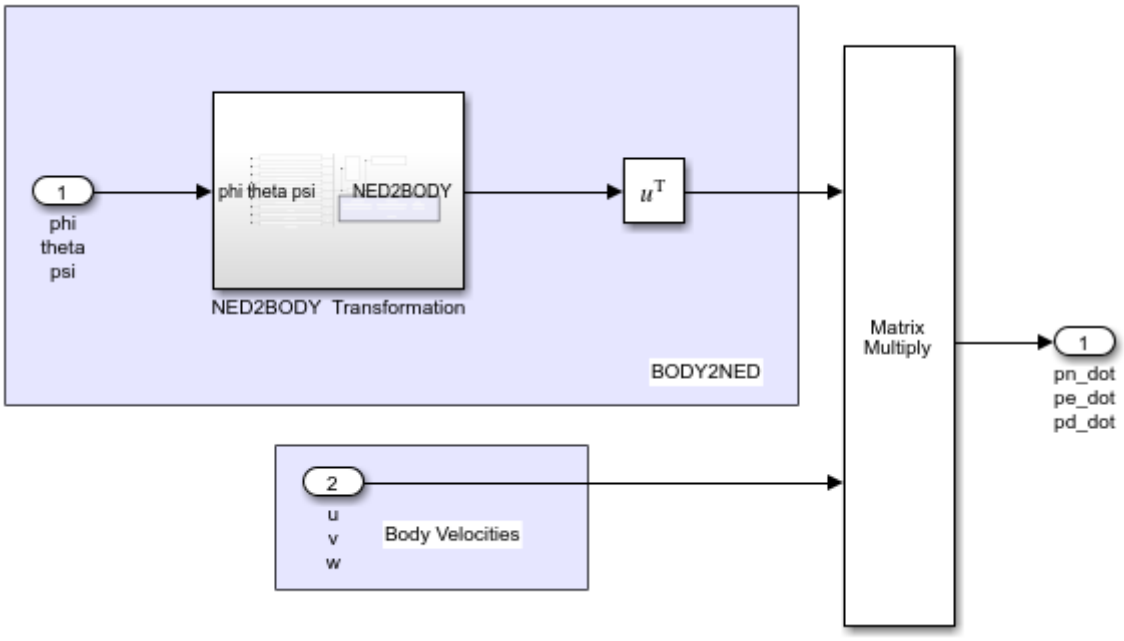

Figure 28. The Simulink Implementation Of Angular Rates Equations

In **Figure 29**, body frame to inertia frame transformation can be seen. This block provide transformation from body frame to inertia frame. Because, while velocities are in body frame, positions are in inertia frame. Inside of this block can be seen in **Figure 29**.

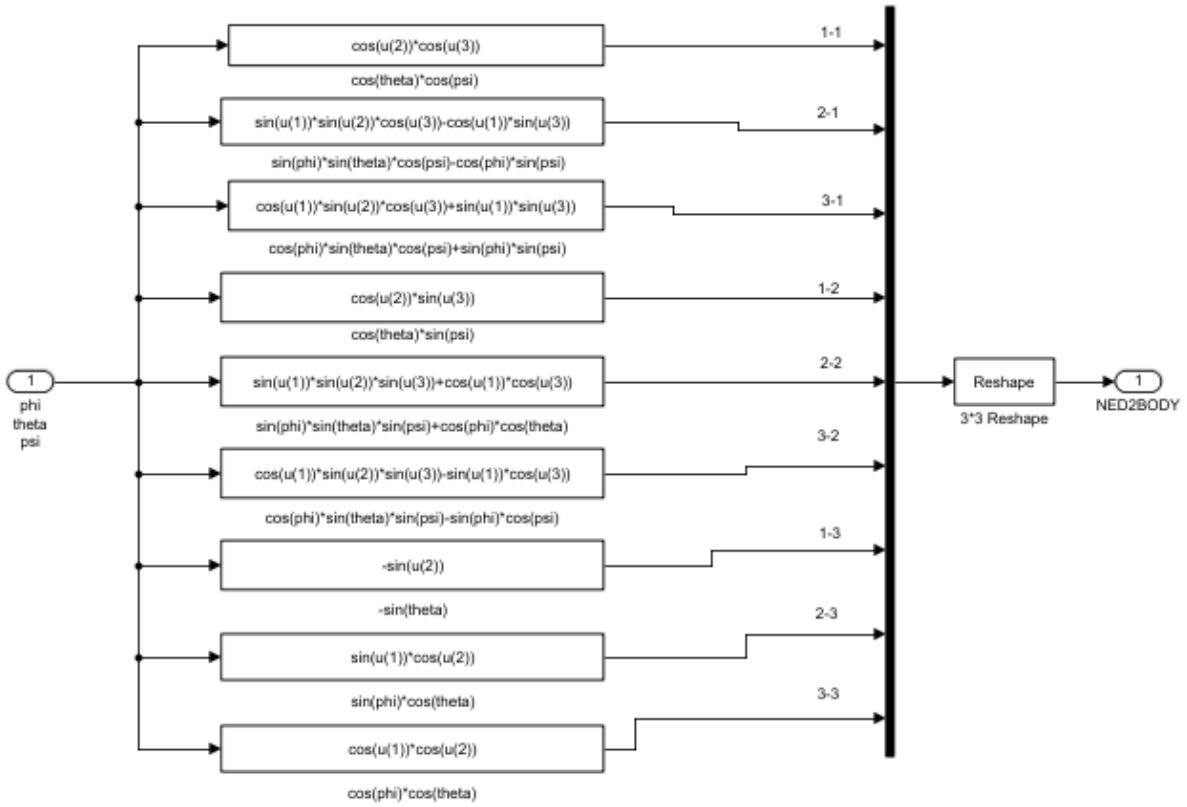

Figure 29. Inside Of NED to Body Block

Body frame to inertia frame transformation matrix was previously shown in Chapter 3, Frames and Axis Transformation title. Besides recalling can be usefull that transpose of body frame to inertia frame transformation matrix is equal with inertia frame to body frame transformation matrix.

4.2.3.5 Wind Frame Components

When aircraft is modeled, wind frame component is always used rather than body velocities. Therefore transformation from body velocities to wind frame component was made and this process was given Equation X1, X2, X3.

$$\alpha = tan^{-1}(\frac{w}{u})$$

$$\beta = sin^{-1}(\frac{v}{V_t})$$

$$V_t = \sqrt{u^2 + v^2 + w^2}$$

$$\dot{V}_t = \frac{\dot{u} * u + \dot{v} * v + \dot{w} * w}{V_t}$$

$$\dot{\alpha} = \frac{\dot{u} * w - \dot{w} * u}{u^2 + w^2}$$

$$\dot{\beta} = \frac{V_t * \dot{v} - \dot{V}_t * v}{{V_t}^2 * \sqrt{1 - \left(\frac{v}{V_t}\right)^2}}$$

The Simulink implementation of body velocities to wind component transformation is shown in **Figure 30**.

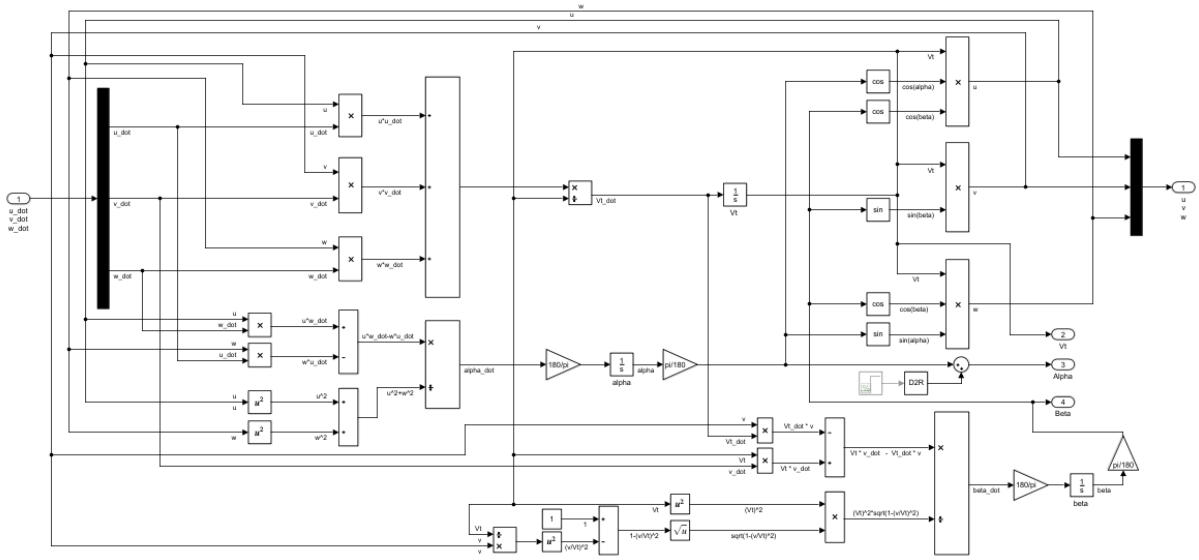

Figure 30. The Simulink implementation of body velocities to wind component transformation

4.3 Flight Gear Simulation

Flight Gear is an open source flight simulator and it can be downloaded from Flight Gear website. It supports a variety of popular platforms (Windows, Mac, Linux, etc.) and it can be used with Simulink environment. While Flight Gear simulation block is used, 6 states are taken from 6-DOF EOM which are 3 positions and 3 attitude angles. Likewise WGS84 Gravity Model, Flight Gear block also takes as inputs 3 geodetic position of aircraft latitude, longitude and altitude. Therefore, 3 inertial positions are converted into geodetic positions by using Flat Earth to LLA block. How does this block used was explained previously in Gravity Model. The Flight Gear Simulation Block also takes 3 attitude angle roll angle, pitch angle and yaw angle. By using these 6 states it simulates aircraft and flight as 3-D. Figure X shows implementation of Flight Gear Simulation subsystem in Simulink. And also in Figure X1, X2 and X3 some views of flight are showed.

5 STABILITY AUGMENTATION SYSTEM DESIGN

In this section stability augmentation system is designed for both longitudional and lateral motion with root locus method. To do this, proper feedback gain was obtained and system stability characteristics were increased.

5.1 Linearizing and Trim

In previous chapter aircraft was modeled as nonlinear but nonlinear aircraft control is more complex and difficult. So it is a convenient solution that linearizing aircraft motion and finding a trim point. At this point control system design can be applied. To linearize aircraft, there are multiple methods like small perturbation theory and linear control anaylsis tool of Matlab. In this thesis linear analysis tool was used and trim point was choosen as 700 ft/s and 15000 ft. To obtain a wing level flight condition trim conditions as properly. Trim results of aircraft was given in **Figure 31.** To obtain this results pilot commands as throttle, elevator, aileron and rudder deflections also can be seen in **Figure 32**. It must be noticed that all angles are in radian.

Edit: op_trim4

Optimizer Output | Details

State | Input | Output

State	Desired Value	Actual Value	Desired dx	Actual dx
B747/Aircraft Dynamics /6-DOF EOM/Wind Frame States/Vt				
State - 1	700	700	0	-3.3323e-12
B747/Aircraft Dynamics /6-DOF EOM/Wind Frame States/alpha				
State - 1	[-Inf , Inf]	0.049552	0	3.1531e-16
B747/Aircraft Dynamics /6-DOF EOM/Wind Frame States/beta				
State - 1	[-Inf , Inf]	0.011327	0	-2.1387e-15
Rates				
State - 1	[-Inf , Inf]	-2.3605e-23	0	9.3134e-13
State - 2	[-Inf , Inf]	-2.9148e-23	0	-5.7919e-15
State - 3	[-Inf , Inf]	-4.3234e-24	0	7.5605e-14
Attitude				
State - 1	[-Inf , Inf]	0.023153	0	-2.3854e-23
State - 2	[-Inf , Inf]	0.049801	0	-2.904e-23
State - 3	[-Inf , Inf]	-1.951e-16	0	-5.0033e-24
Position				
State - 1	[-Inf , Inf]	-8.1392e-19	[-Inf , Inf]	699.9638
State - 2	[-Inf , Inf]	1.1683e-16	[-Inf , Inf]	7.1236
State - 3	-15000	-15000	0	2.1949e-11

Initialize model...

Figure 31.

Edit: op_trim4

Optimizer Output | Details

State | Input | Output

Input	Desired Value	Actual Value
B747/Input		
Input - 1	[0 , 1]	0.37292
B747/Input1		
Input - 1	[-0.40143 , 0.29671]	0.065637
B747/Input2		
Input - 1	[-0.34907 , 0.34907]	0.051645
B747/Input3		
Input - 1	[-0.34907 , 0.34907]	0.020101

Figure 32

With this trim conditions aircraft pilot inputs and all states can be seen in Figure X.

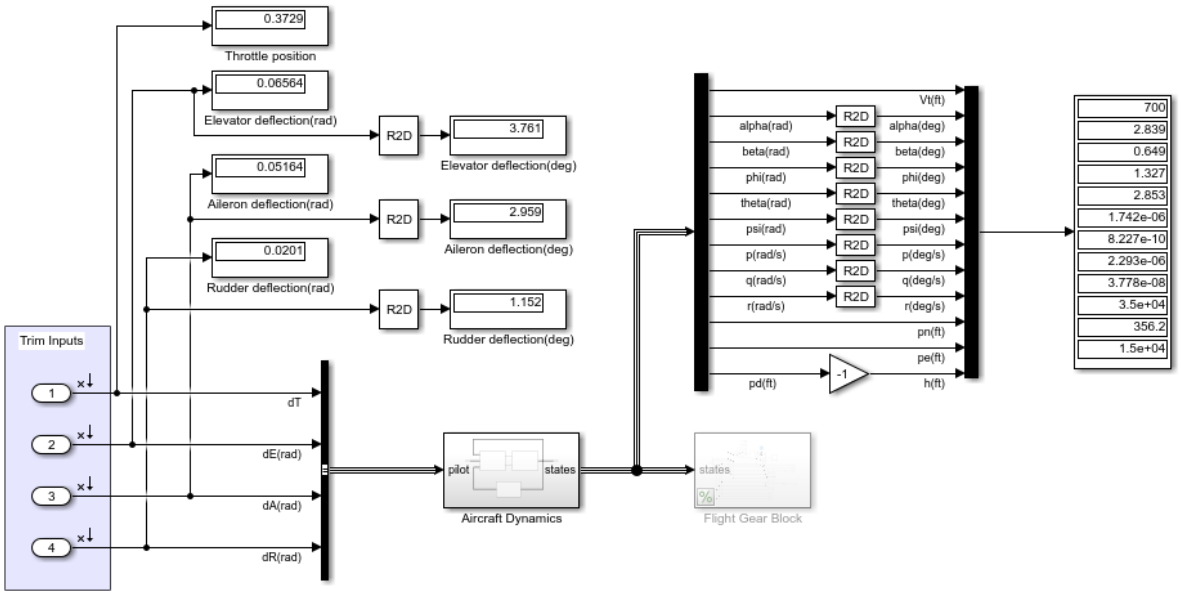

Figure 33

5.2 Root Locus Design Method

After linearization, four transfer function were obtained to investigate and improve longitudional and lateral stability characteristics. These functions are alpha to elevator deflection, pitch rate to elevator deflection, roll rate to aileron deflection and yaw rate to rudder deflection transfer functions.

The root locus method is used in this thesis to analyse and improve system response. The root locus plot for each transfer function was plotted and by choosing proper feedback gain, SAS design was applied.

5.3 Longitudional Stability Augmentation System Design

5.3.1 Pitch Damper

In previous section aircraft was linearized and trimmed at a specific point. In this section by using linear control analysis tool four transfer function were obtained. First transfer function is alpha to elevator deflection transfer function was given below.

$$\frac{a}{\delta_e} = \frac{-0.04555s^3 - 1.926s^2 - 0.01098s - 0.008851}{s^4 + 1.485s^3 + 2.788s^2 + 0.01904s + 0.01354}$$

Impulse response of this transfer function can be seen in Figure X. As can be seen in figure the response is stable but whether there is any better response is investigated.

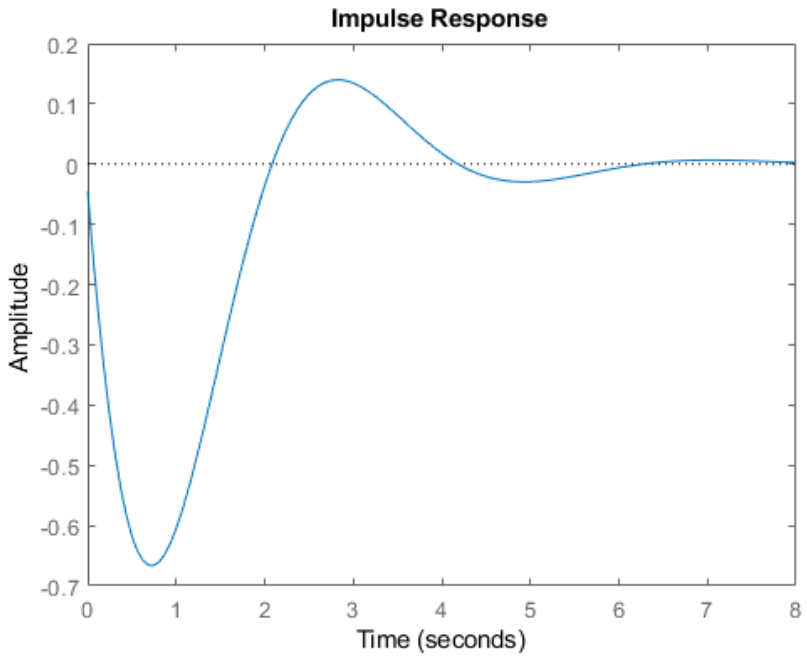

Figure 34

By using alpha to elevator transfer function root locus plot is drawn. It can be seen in Figure X.

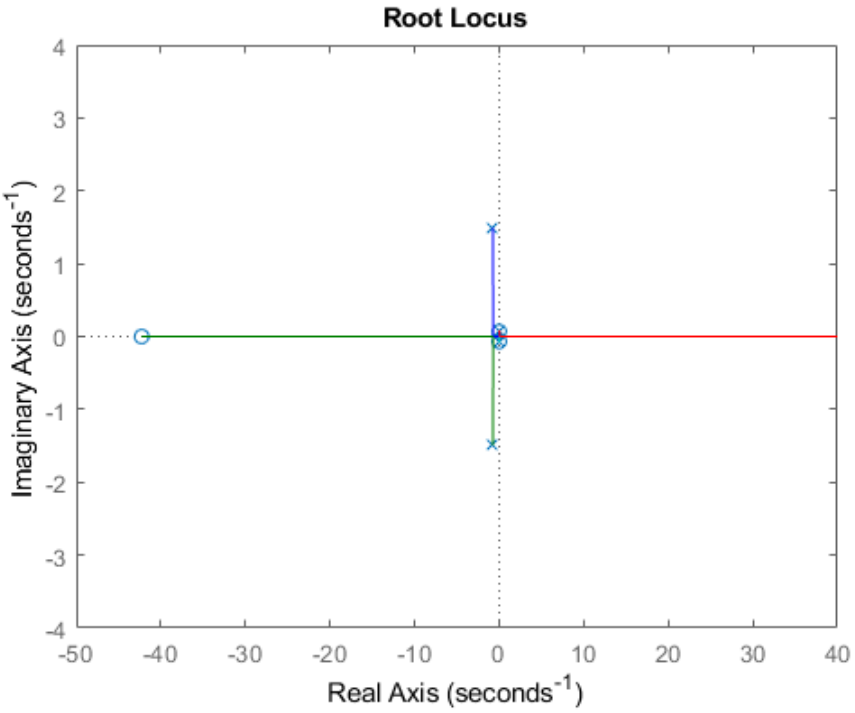
Root Locus
Imaginary Axis (seconds-1)
Real Axis (seconds-1)
4
3
2
1
0
-1
-2
-3
-4
-50
-40
-30
-20
-10
0
10
20
30
40

Figure 35

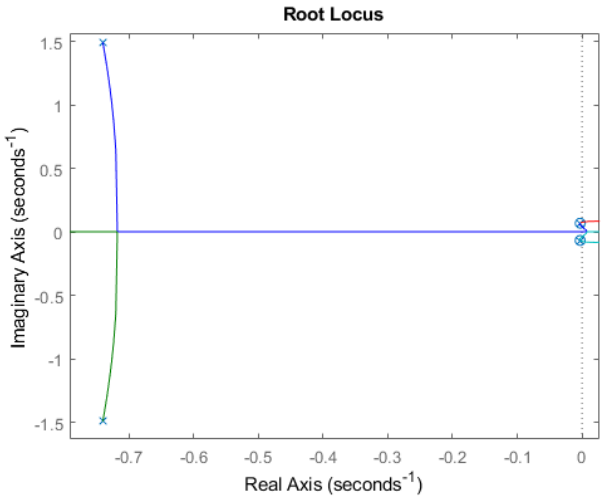
Root Locus
Imaginary Axis (seconds-1)
Real Axis (seconds-1)
1.5
1
0.5
0
-0.5
-1
-1.5
-0.7
-0.6
-0.5
-0.4
-0.3
-0.2
-0.1
0

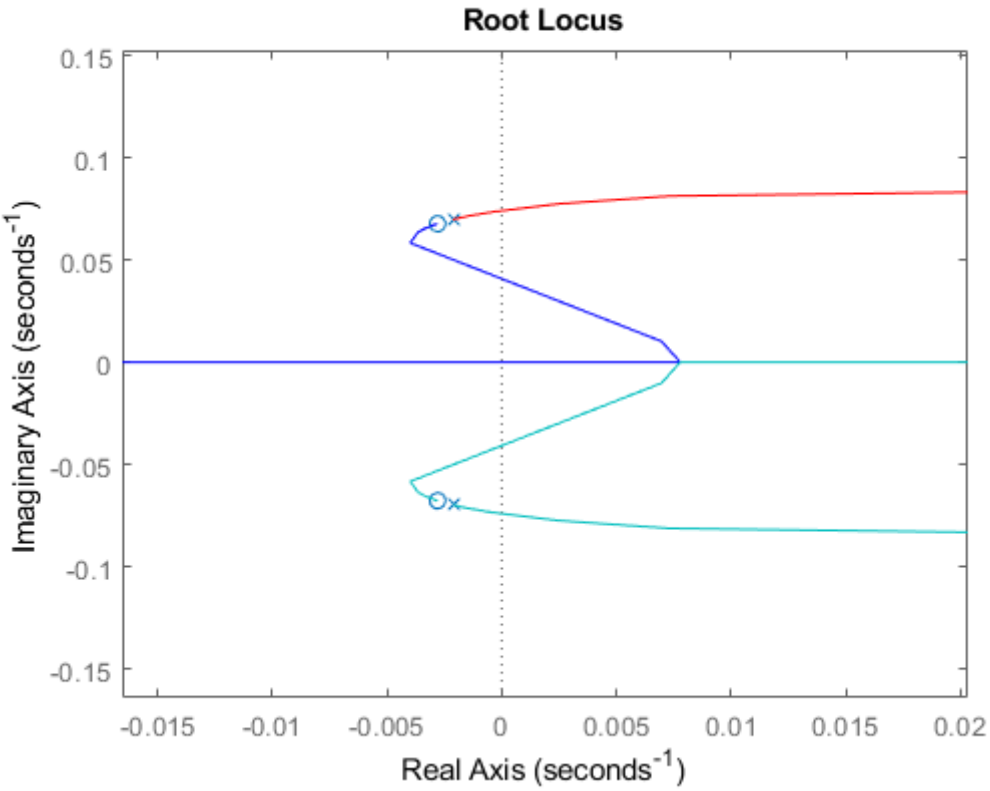

As can be seen in figure X, two poles at left are faster and those are short period poles, right two poles are slower and those are phugoid poles. While proper feedback gain are choosen slower poles are more important, because faster poles are rapidly settled to stable condition. As can be seen in Figure X, when gain is investigated for slower poles, as gain increase system response is become unstable. So K_a is choosed as 0,in an another saying there is no feedback for alpha response. Alpha response could not be improved by using alpha feedback, but pitch rate feedback also improved alpha response later on.

$$\frac{q}{\delta_e} = \frac{-1.924s^3 - 1.527s^2 - 0.01504s + 5.372e - 19}{s^4 + 1.485s^3 + 2.788s^2 + 0.01904s + 0.01354}$$

Impulse response of this transfer function can be seen in Figure X. As can be seen in figure the response is stable but whether there is any better response is investigated.

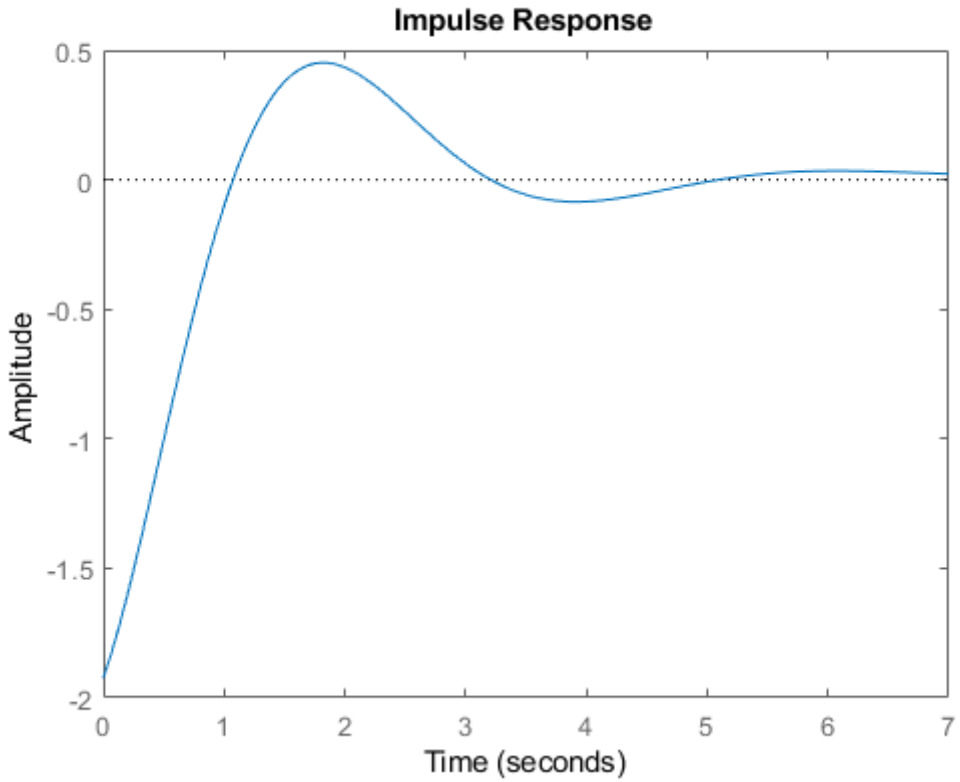

Figure 36

By using pitch rate to elevator transfer function, root locus plot was drawn. As can be seen in Figure X, when root locus plot examined, any positive gain gave no better response. So negative feedback gain was attempted. Negative transfer function root locus can be seen in Figure X. By examining negative transfer function root locus K_q was choosed as -0.9. At this gain value damping ratio is approximately 0.7.

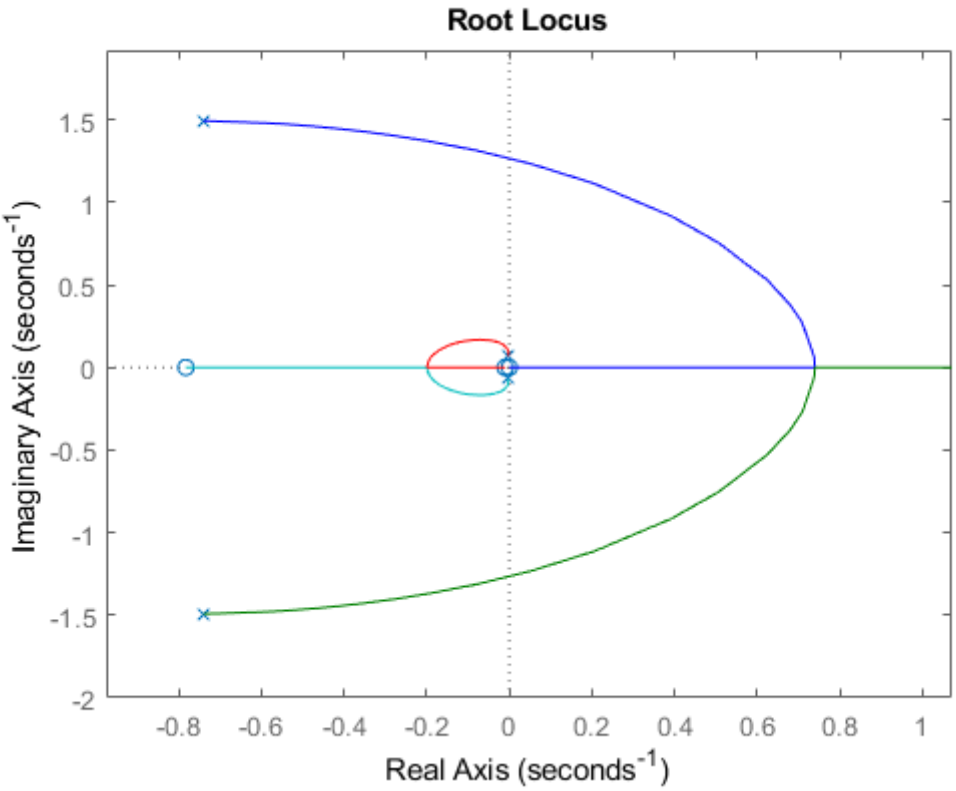

Figure 37

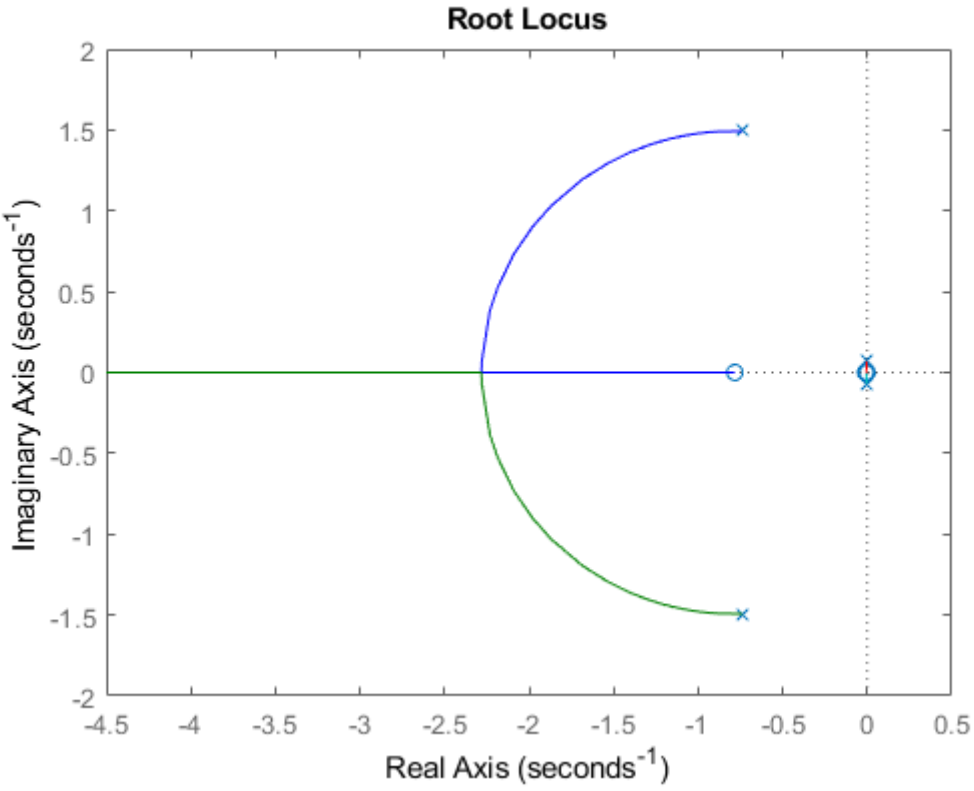

Figure 38

It can be seen in Figure X, there is an improvement in impulse response compares to without feedback impulse response situation.

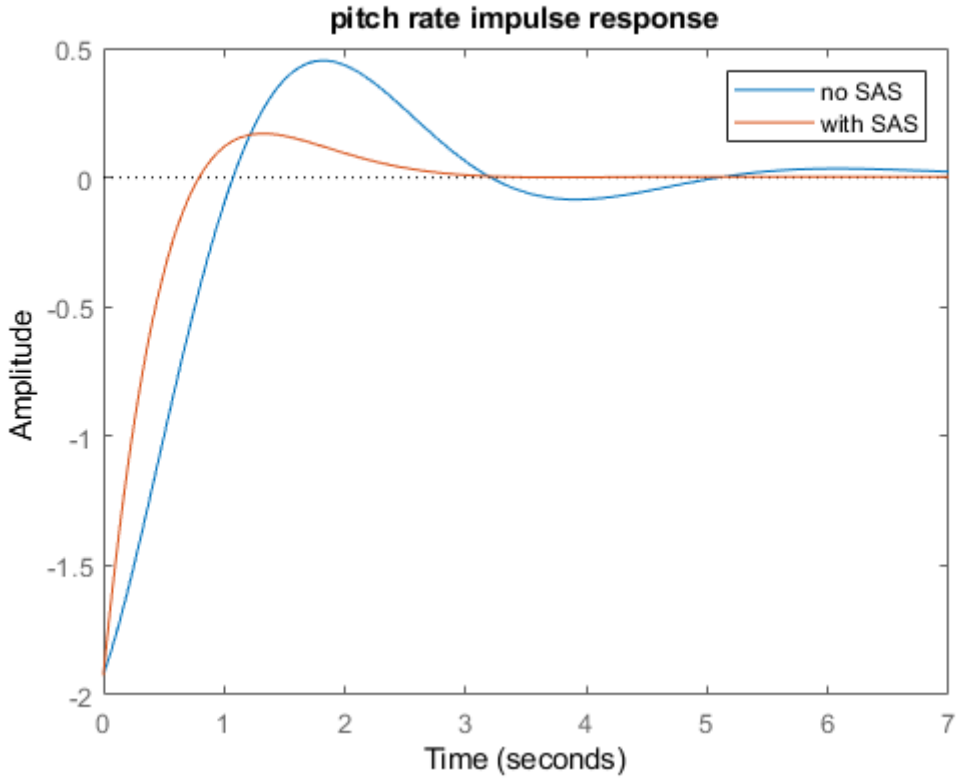

Figure 39

As can be seen in Figure X, with pitch rate feedback, impulse response of alpha improved. Its oscillation decreased and settling time decrease.

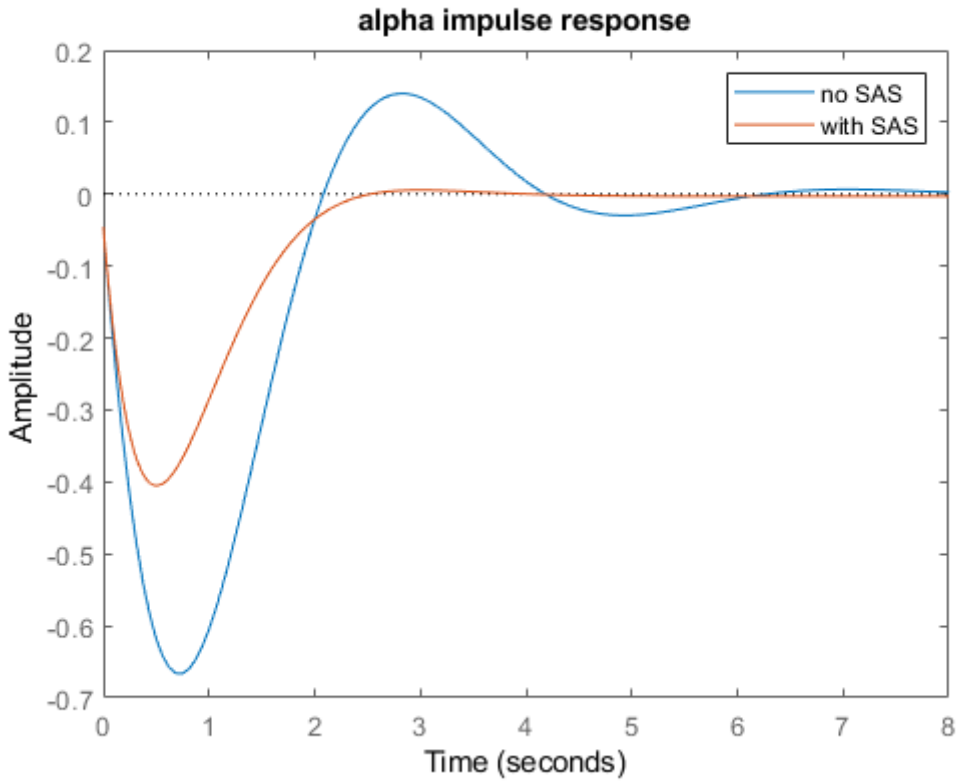

Figure 40

5.4 Lateral Stability Augmentation System Design

5.4.1 Roll Damper

Roll rate to aileron deflection transfer function was found as:

$$\frac{p}{\delta_a} = \frac{0.6932s^3 + 2.872\,s^2 + \ 1.518s - \ 0.00258}{s^4 + 334.9s^3 + 133.4s^2 + \ 498.1 - \ 7.255}$$

Impulse response of this transfer function can be seen in Figure X. As can be seen in figure response is stable. With root locus method, whether any better response is exist was investigated.

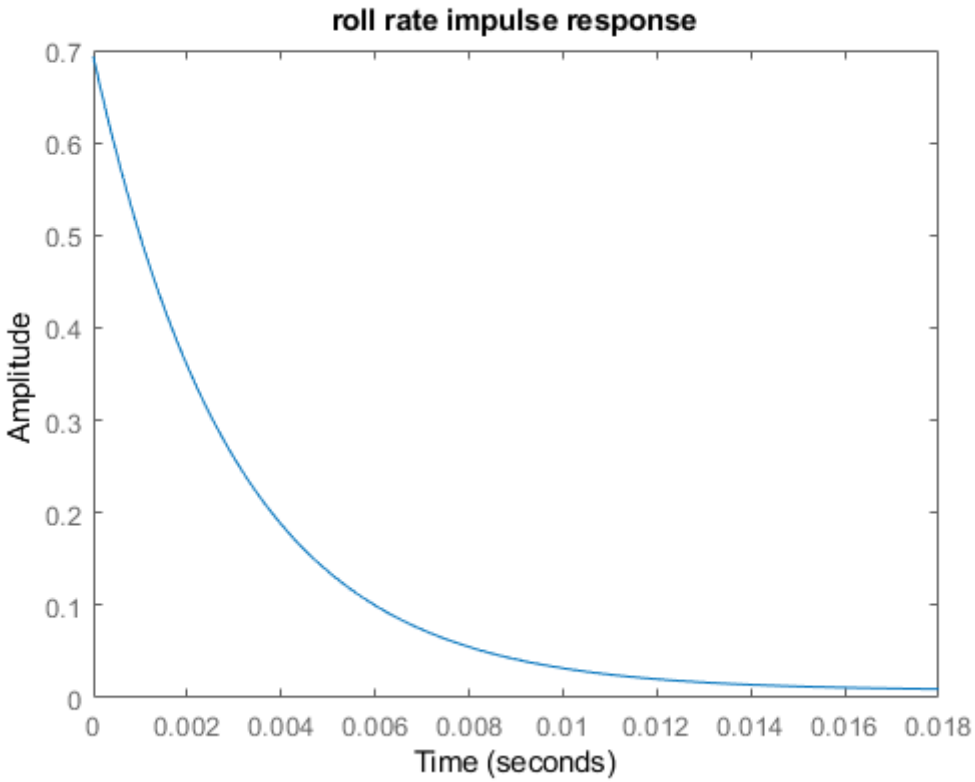

Figure 41

By using roll rate to aileron deflection transfer function, root locus plot was obtained. As can be seen in Figure X, one pole is highly fast and it is located approximately -350. This pole was ignored and design was made by using slower root which are located near to imaginer axis. As a result of gain investiagation K_p was choosen as 219 and damping ratio is 0.8.

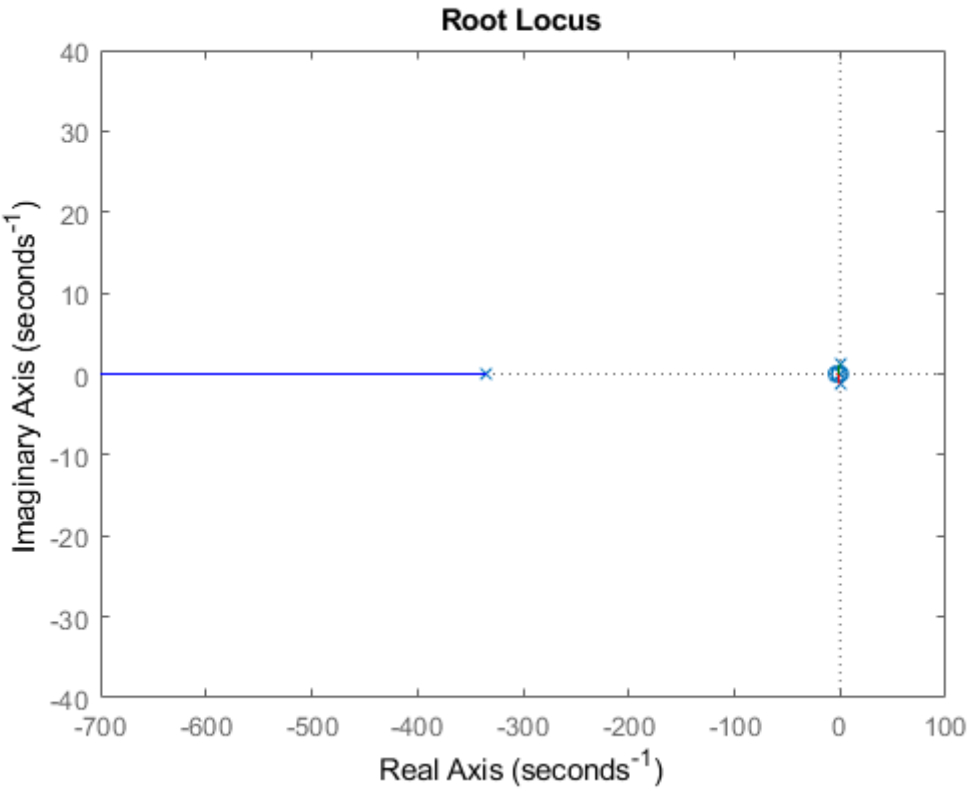

Figure 42

With Kp feedback step response of roll rate can be seen in Figure X. Comparison between response with and without feedback also shown in Figure.

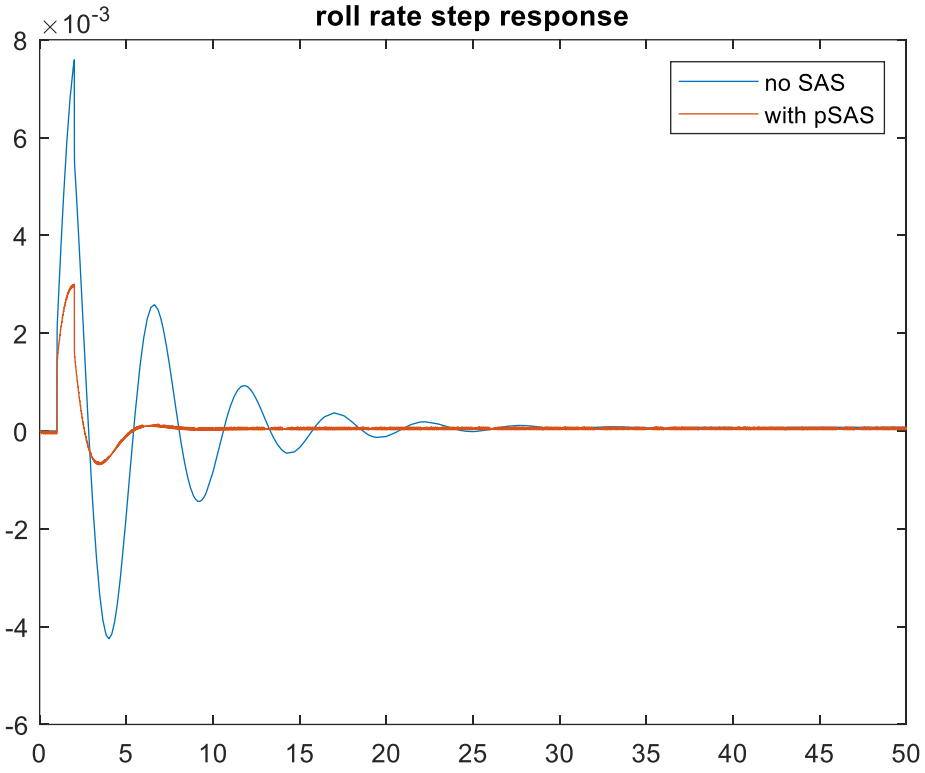

Figure 43

Figure X show that any feedback for roll rate impact yaw rate directly. As can be seen in figure Kp gain also improved yaw rate step response.

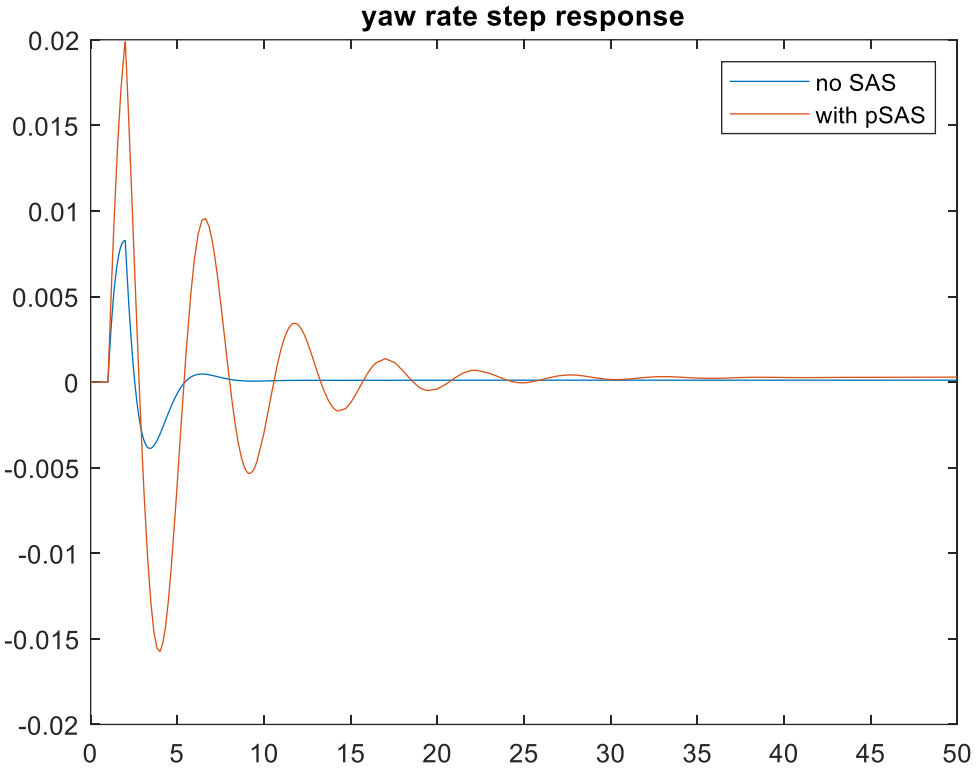
yaw rate step response
no SAS
with pSAS
0.02
0.015
0.01
0.005
0
-0.005
-0.01
-0.015
-0.02
0
5
10
15
20
25
30
35
40
45
50

Figure 44

5.4.2 Yaw Damper

Finally the last transfer function, yaw rate to rudder deflection is that:

$$\frac{r}{\delta_r} = \frac{-0.8973s^3 - 304.4\,s^2 - 29.85s - 0.1311}{s^4 + 334.9s^3 + 133.4s^2 + 498.1 - 7.255}$$

Impulse of this transfer function can be seen in Figure X. As can be seen in figure, response is stable. But any faster and more damped response can be exist.

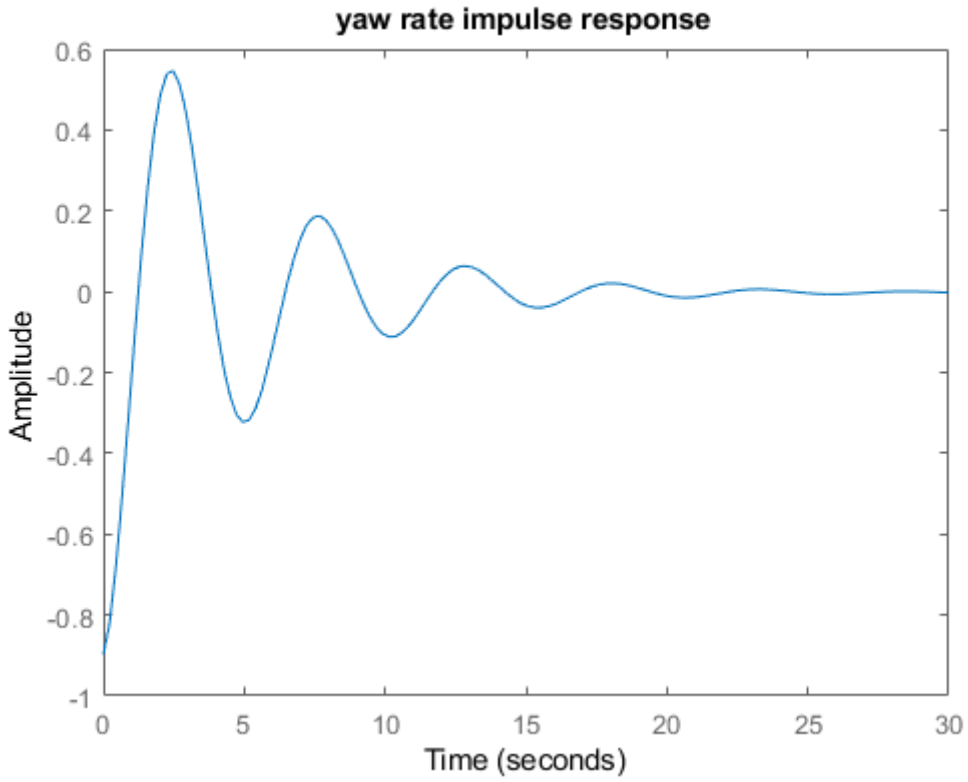

Figure 45

If root locus plot of this transfer function is drawn, it can be seen one root is located as approximately -330. So near to the imaginer axis roots are investigated and any better response can not be found. Thus, negative feedback gain was attempted.

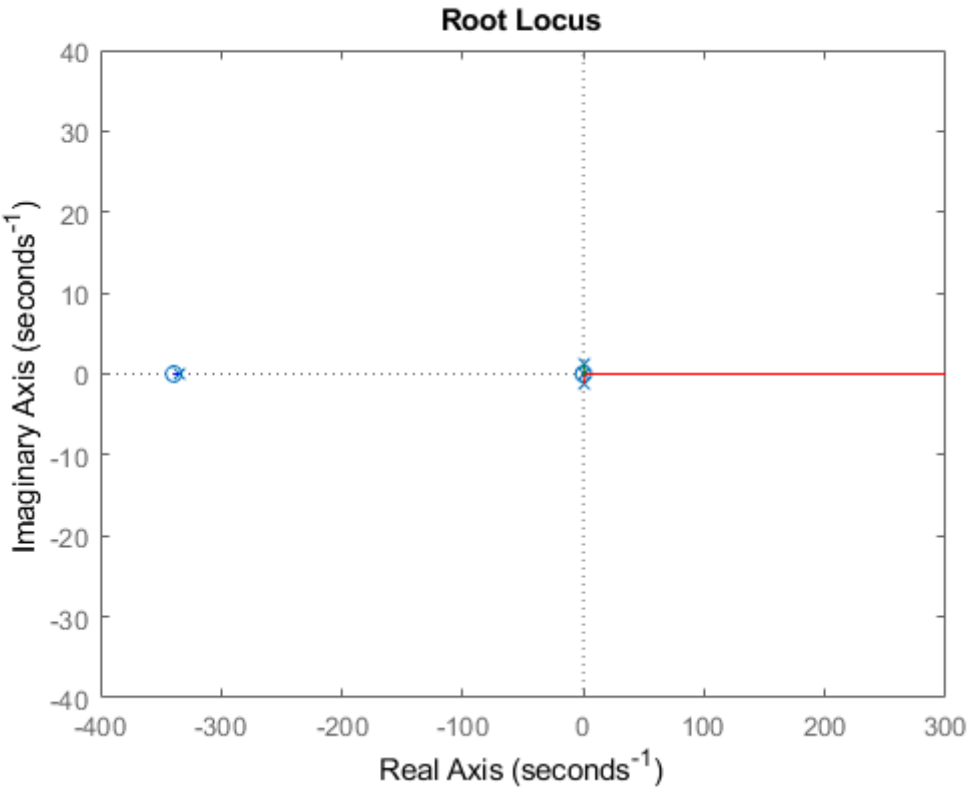

Figure 46

As it can be seen in Figure X, root locus plot of negative transfer function was drawn and near to the imaginer axis roots were investigated. As a result of investigation K_r is choosed as -1.8

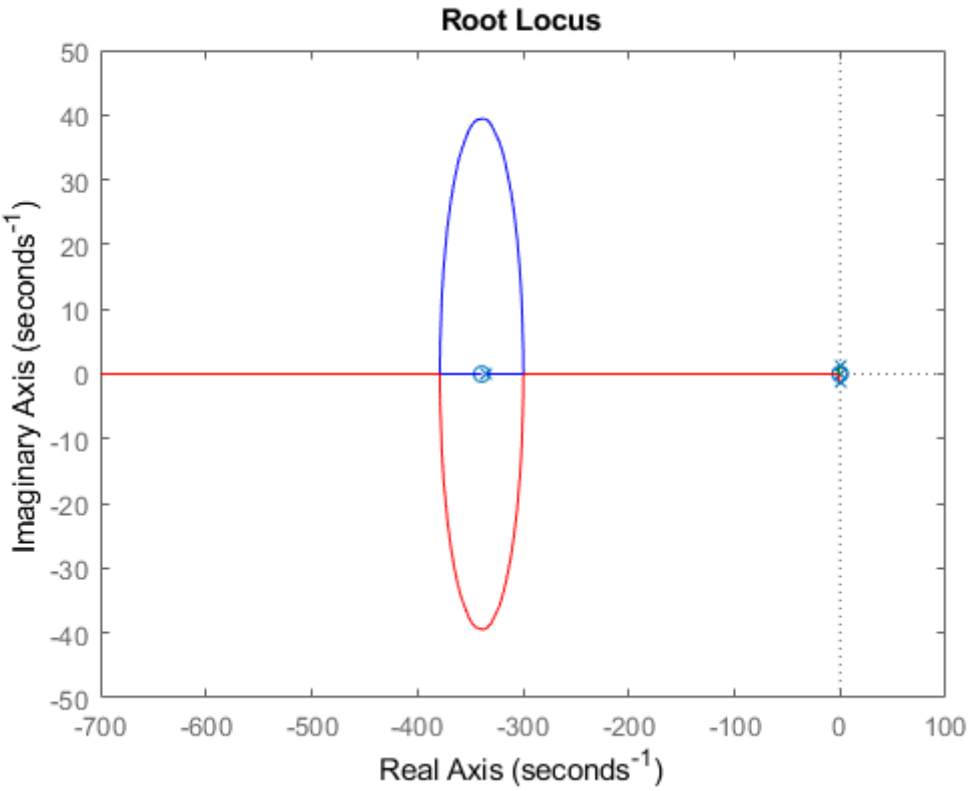

Figure 47

An improvement in yaw and roll rate step responses can be seen in Figure X and X1. Although main purpose of yaw damper, is improve yaw rate response, because of lateral and directional motion is coupled, roll rate response was also improved.

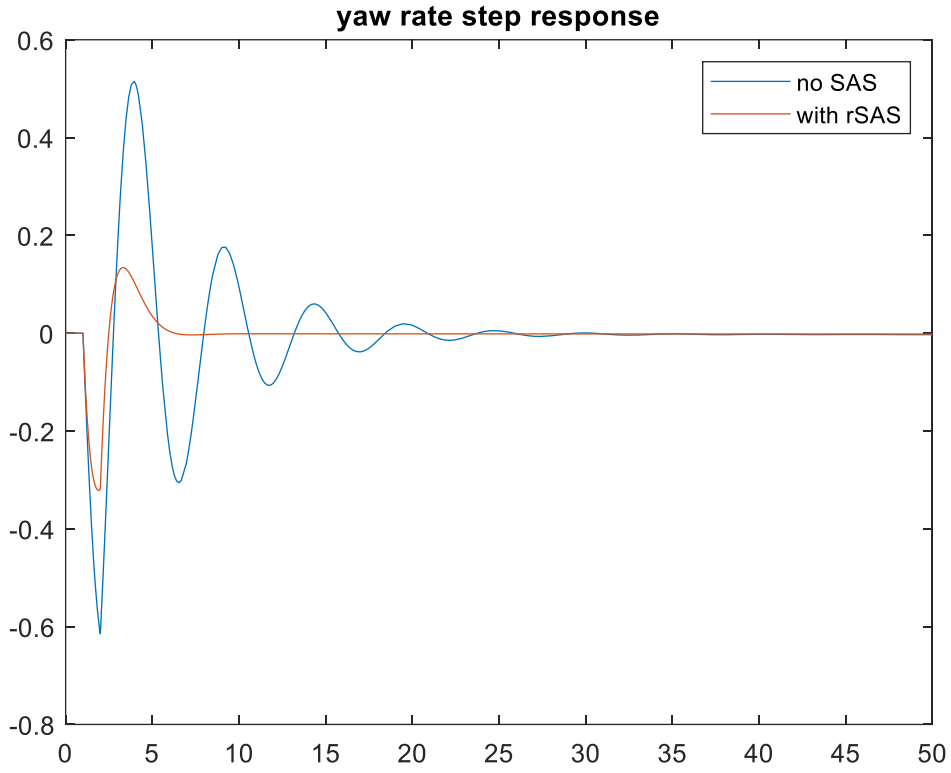

Figure 48

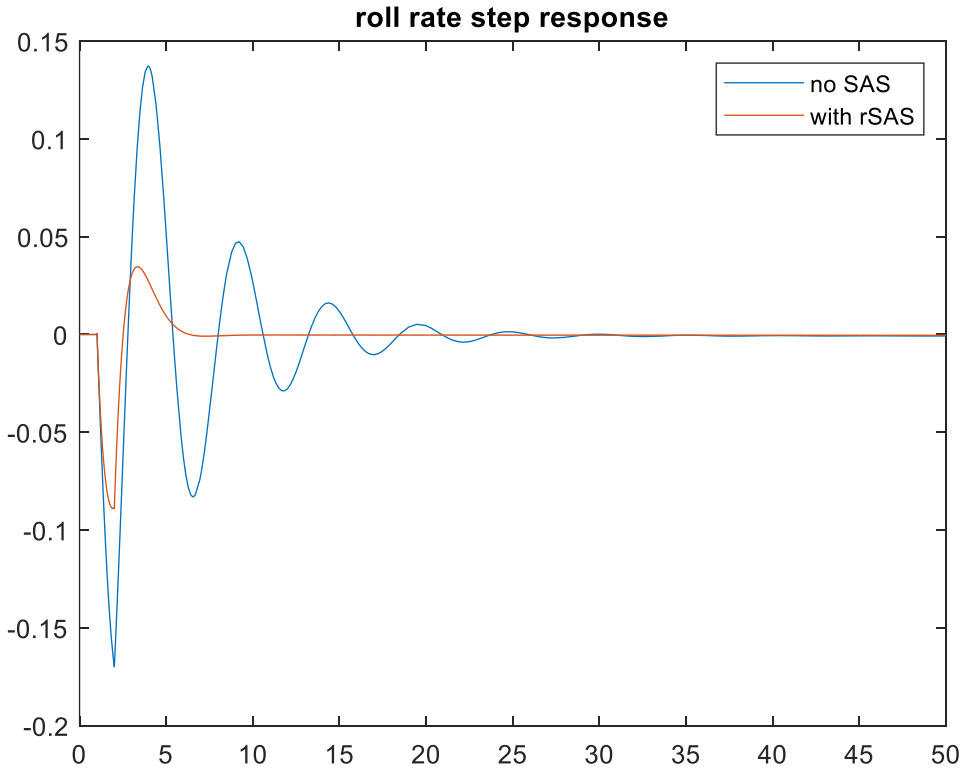

Figure 49

Overall demonstration of model with SAS design can be seen in Figure X.

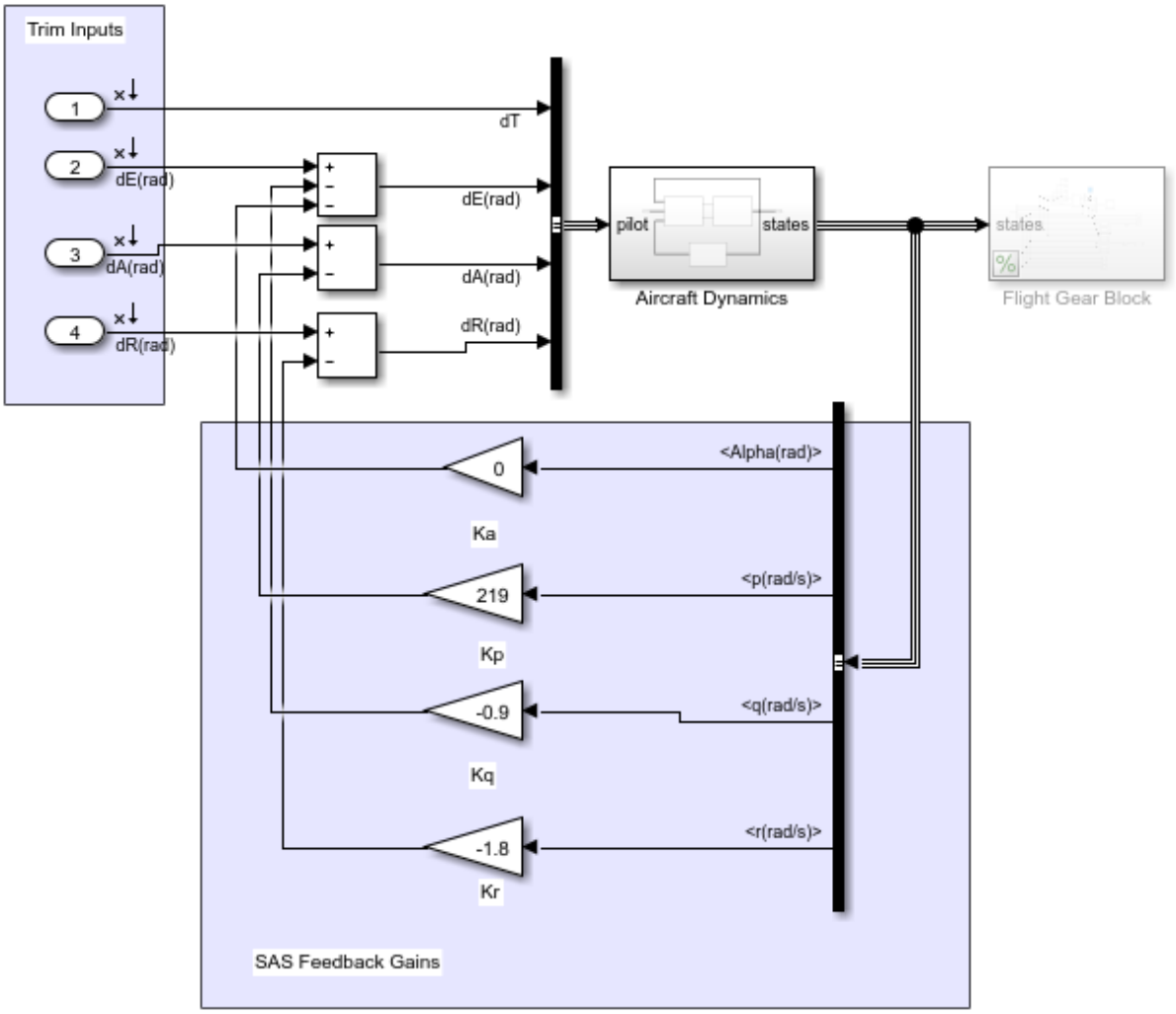

Figure 50

6 REFERENCES

Hanke, C. R., and Nordwall, D. R., “The Simulation of a Jumbo Jet Transport Aircraft” Volume 1 and 2, The Boeing Company, Wichita, Kansas, March 1971.

Kılıç, M. C., “Aircraft Dynamical Modelling and Simulation” , 2008.

Etkin, B., Reid, L., D., *Dynamics of Flight,* John Wiley,1996.

Nelson, R., C., *Flight Stability and Automatic Control*, McGrawHill, 1998.

Stevens, B. L. And Lewis, L. F., *Aircraft Control and Simulation*, John Wiley, Hoboken NJ, 2003.

Kumbasar, S.,’ Design and Development of a Boeing 747 Simulator Mathematical Model’,2012.

Beard, R.W. and McLain, T.W. (2012). Small Unmanned Aircraft: Theory and Practice, Princeton University Press.